Photoinduced Generation of Catalytic Complexes from Substituted-Titanocene−Bis(trimethylsilyl)ethyne Complexes: Contribution to the Mechanism of the Catalytic Head-to-Tail Dimerization of Terminal Alkynes

Petr Štěpnička, Róbert Gyepes, and Ivana Císařová

Department of Inorganic Chemistry, Charles University, Hlavova 2030, 128 40 Prague 2, Czech Republic

Michal Horáček, Jiří Kubišta, and Karel Mach*

J. Heyrovský Institute of Physical Chemistry, Academy of Sciences of the Czech Republic, Dolejškova 3, 182 23 Prague 8, Czech Republic

Received July 13, 1999

A number of substituted-titanocene−alkynyl−alkenyl complexes, [(η^5-$C_5Me_4R^1$)$_2$Ti(η^1-C≡CR^2)(η^1-(*E*)-CH=CHR^2)] (R^1 = H, Me, Ph, Bz; R^2 = CMe_3, $SiMe_3$, ferrocenyl; **A** type complexes), were obtained by reacting the corresponding bis(trimethylsilyl)ethyne complexes [(η^5-$C_5Me_4R^1$)$_2$Ti(η^2-$Me_3SiC{\equiv}CSiMe_3$)] with 1-alkynes $R^2C{\equiv}CH$ in the dark at 60 °C. The complexes undergo a coupling of the carbyl ligands upon exposure to sunlight to give titanocene complexes with 1,4-disubstituted but-1-en-3-ynes, [(η^5-$C_5Me_4R^1$)$_2$Ti(3,4-η-$R^2C{\equiv}CCH{=}CHR^2$)] (**B** type complexes). In contrast to **A** type complexes that do not react further with an excess of *tert*-butylethyne and (trimethylsilyl)ethyne in the dark, **B** type complexes induce rapid dimerization of these terminal alkynes to 2,4-disubstituted but-1-en-3-ynes (head-to-tail dimers). This implies that the known dimerization of 1-alkynes in the presence of [(η^5-$C_5Me_4R^1$)$_2$Ti(η^2-$Me_3SiC{\equiv}CSiMe_3$)] (R^1 = H, Me) performed in diffuse daylight is initiated by the **B** type complexes originating from photoinduced conversion of the initially formed **A** type products. Titanocene complexes with 2,4-disubstituted but-1-en-3-ynes, [(η^5-$C_5Me_4R^1$)$_2$Ti(3,4-η-$R^2C{\equiv}CC(R^2){=}CH_2$)] ($R^1$ = H, Me, Ph; R^2 = $SiMe_3$), were also prepared and their participation in the catalytic cycle was demonstrated.

Introduction

Linear dimerizations of terminal acetylenes are catalyzed by various organometallic complexes of early,[1] first-row,[2] and late[3] transition metals as well as by complexes of rare-earth metals, lanthanides, and actinides,[4] affording 2,4-disubstituted but-1-en-3-ynes (head-to-tail or HTT dimers), 1,4-disubstituted but-1-en-3-ynes (head-to-head or HTH dimers), and 1,4-disubstituted buta-1,2,3-trienes. Among the numerous catalysts, decamethyltitanocene-derived systems produce HTT dimers with an astonishing selectivity.[1a] The turnover numbers (TN) (0.5−1.2) × 10^3 and a selectivity to HTT dimers of around 99% were achieved for (trimethylsilyl)ethyne (TMSE), propyne, 1-butyne, 1-pentyne, 1-hexyne, and cyclohexylethyne using either the [(η^5-C_5Me_5)$_2$$TiCl_2$]/*i*-PrMgCl/ether (ether = Et_2O, THF) systems[5] or the [(η^5-C_5Me_5)$_2$Ti(η^2-$Me_3SiC{\equiv}CSiMe_3$)] complex[6] as the catalyst precursor. Although *tert*-butylethyne (TBUE) was found to be unreactive toward all the above catalysts,[1a,5,6] it is dimerized to its HTT dimer by the [(η^5-C_5Me_4H)$_2$$TiCl_2$]/*i*-PrMgCl/THF catalytic system or the [(η^5-C_5Me_4H)$_2$Ti(μ-H)$_2$Mg(μ-Cl)]$_2$ complex, the TN value (∼8.8 × 10^3) appearing to have been limited by trace amounts of *tert*-butyl alcohol in

* To whom correspondence should be addressed. E-mail: mach@jh-inst.cas.cz.

(1) (a) Ti: Akita, H.; Yasuda, H.; Nakamura, A. *Bull. Chem. Soc. Jpn.* **1984**, *57*, 480. (b) Zr: Horton, A. D. *J. Chem. Soc., Chem. Commun.* **1992**, 185. (c) Hf: Yoshida, M.; Jordan, R. F. *Organometallics* **1997**, *16*, 4508.

(2) (a) Cr: Hagihara, N.; Tamura, M.; Yamazaki, H.; Fujiwara, M. *Bull. Chem. Soc. Jpn.* **1961**, *34*, 892. (b) Cu: Akhtar, M.; Richards, T. A.; Weedon, B. C. L. *J. Chem. Soc.* **1959**, 933. (c) Cu: Balcioğlu, N.; Uraz, I.; Bozkurt, C.; Sevin, F. *Polyhedron* **1997**, *16*, 327.

(3) (a) Ru: Wakatsuki, Y.; Yamazaki, H.; Kumegawa, N.; Satoh, T.; Satoh, J. Y. *J. Am. Chem. Soc.* **1991**, *113*, 9604. (b) Ru: Yo, C. S.; Liu, N. *Organometallics* **1996**, *15*, 3968. (c) Ru: Slugovc, C.; Mereiter, K.; Zobetz, E.; Schmid, R.; Kirchner, K. *Organometallics* **1996**, *15*, 5275. (d) Rh: Schäfer, M.; Mahr, N.; Wolf, J.; Werner, H. *Angew. Chem., Int. Ed. Engl.* **1993**, *32*, 1315. (e) Rh: Kovalev, I. P.; Yevdakov, K. V.; Strelenko, Yu. A.; Vinogradov, M. G.; Nikishin, G. I. *J. Organomet. Chem.* **1990**, *386*, 139. (f) Pd: Trost, B. M.; Sorum, M. T.; Chan, C.; Harms, A. E.; Rühter, G. *J. Am. Chem. Soc.* **1997**, *119*, 698. (g) Os: Barbaro, P.; Bianchini, C.; Peruzzini, M.; Polo, A.; Zanobini, F.; Frediani, P. *Inorg. Chim. Acta* **1994**, *220*, 5. (h) Ir: Jun, C.-H.; Lu, Z.; Crabtree, R. H. *Tetrahedron Lett.* **1992**, *47*, 7119.

(4) (a) Sc: Thompson, M. E.; Baxter, S. M.; Bulls, A. R.; Burger, B. J.; Nolan, M. C.; Santarsiero, B. D.; Schaefer, W. P.; Bercaw, J. E. *J. Am. Chem. Soc.* **1987**, *109*, 203. (b) Y: den Haan, K. H.; Wielstra, Y.; Teuben, J. H. *Organometallics* **1987**, *6*, 2053. (c) Y: Schaverien, C. J. *Organometallics* **1994**, *13*, 69. (d) Ce: Heeres, H. J.; Nijhoff, J.; Teuben, J. H.; Rogers, R. D. *Organometallics* **1993**, *12*, 2609. (e) Th, U: Hasket, A.; Wang, J. Q.; Straub, T.; Neyroud, T. G.; Eisen, M. S. *J. Am. Chem. Soc.* **1999**, *121*, 3025. (f) Th, U: Straub, T.; Haskel, A.; Eisen, M. S. *J. Am. Chem. Soc.* **1995**, *117*, 6364. (g) U: Wang, J. Q.; Dash, A. K.; Berthet, J. C.; Ephritikhine, M.; Eisen, M. S. *Organometallics* **1999**, *18*, 2407.

(5) Varga, V., Petrusová, L.; Čejka, J.; Mach, K. *J. Organomet. Chem.* **1997**, *532*, 251.

(6) Varga, V., Petrusová, L.; Čejka, J.; Hanuš, V.; Mach, K. *J. Organomet. Chem.* **1996**, *509*, 235.

10.1021/om9905714 CCC: $18.00
Publication on Web 10/16/1999

TBUE, which deactivates the catalyst.[7] Investigations of the above titanocene dichloride−Grignard reagent catalytic systems showed that the catalytic species arises from a titanocene diacetylide tweezer complex that contains Mg^{2+} cation embedded between the tweezer acetylide arms. The true catalytic species is to be either a monomeric titanocene acetylide[8] or a titanocene Ti(II) complex generated from the latter compound by an as yet unknown redox reaction.[5] The latter possibility is supported by the fact that all nonpolar 1-alkynes tested (except TBUE) are dimerized to their HTT dimers by [(η^5-C_5Me_5)$_2$Ti(η^2-$Me_3SiC{\equiv}CSiMe_3$)] with similar activities and selectivities. The catalytic cycle of the HTT dimer formation was proposed; however, no products resulting from the reaction of [(η^5-C_5Me_5)$_2$Ti(η^2-$Me_3SiC{\equiv}CSiMe_3$)] with 1-alkynes were isolated and identified.[6] This was mainly due to a slow conversion of this complex to the catalytically active species, whose concentration remained very low during the alkyne dimerization. The validity of the catalytic cycle has recently been brought in doubt by an observation that [(η^5-C_5Me_5)$_2$Ti(η^2-$Me_3SiC{\equiv}CSiMe_3$)] reacts with terminal alkynes to afford the decamethyltitanocene (η^1-(*E*)-alkenyl)(η^1-alkynyl) complexes, which cannot obviously be the precursors of the HTT dimers.[9]

Here we report the formation of [(η^5-$C_5Me_4R^1$)$_2$Ti(η^1-$C{\equiv}CR^2$){η^1-(*E*)-$CH{=}CHR^2$}] complexes from [(η^5-$C_5Me_4R^1$)$_2$Ti(η^2-BTMSE)] (R^1 = H, Me, Ph, Bz (benzyl); BTMSE = bis(trimethylsilyl)ethyne) and alkynes $R^2C{\equiv}CH$ (R^2 = *t*-Bu, $SiMe_3$, Fc (ferrocenyl)), as well as their photoinduced transformation to [(η^5-$C_5Me_4R^1$)$_2$Ti{η^2-(*E*)-$R^2C{\equiv}CCH{=}CHR^2$}] complexes, containing a η^2-coordinated triple bond. Some titanocene complexes with the η^2-coordinated HTT dimer (TMSE)$_2$, [(η^5-$C_5Me_4R^1$)$_2$Ti-{3,4-η-$Me_3SiC{\equiv}CC(SiMe_3){=}CH_2$}] ($R^1$ = H, Me, Ph), which have to be involved in the dimerization reaction, were also prepared, and their reactivity toward selected terminal alkynes has been examined in order to throw more light on the catalytic cycle.

Results and Discussion

The substituted-titanocene−η^2-bis(trimethylsilyl)-ethyne (BTMSE) complexes [(η^5-$C_5Me_4R^1$)$_2$Ti(η^2-$Me_3SiC{\equiv}CSiMe_3$)] (R^1 = H (**1**), Me (**2**), Ph (**3**), Bz (**4**)) react with terminal alkynes such as *tert*-butylethyne (TBUE), (trimethylsilyl)ethyne (TMSE), or ferrocenylethyne (FCE) in a uniform way to yield exclusively (η^1-(*E*)-alkenyl)-(η^1-alkynyl)titanocenes **A1**−**A6** (Scheme 1). The reaction is slow, even at a 20-fold excess of the alkyne, and requires at least several hours to reach completion at 60 °C, as evidenced by following the conversion of the BTMSE complexes through decay of their absorption band at 920 nm.[6] When the reaction is carried out under strict exclusion of light, complexes of the **A** type are formed with no admixture of head-to-tail dimers from either of the alkynes. Compounds **A** are orange-yellow oils or waxy solids, except for **A1**, which was obtained in a crystalline form from a concentrated hexane solution, and the red ferrocene derivative **A6**, which crystallized from its concentrated toluene solution. The structures of **A** type complexes have been determined by ^{1}H and ^{13}C NMR spectroscopy. The ^{1}H NMR spectra are suggestive of a *trans* configuration at the η^1-coordinated carbon−carbon double bond in all cases, as judged from $^3J_{HH}$ values. The ^{13}C NMR spectra (Table 1) are in full accordance with the proposed structures as well but provide much clearer information about the coordination of the hydrocarbyl ligands.[10] The low-field signals observed at δ_C 145−180 and 115−125 belong to the C^α and C^β carbon atoms of the σ-bonded triple bond, whereas those at δ_C 190−225 and 130−145 are due to the σ-bonded double bond (C^α and C^β, respectively).

Scheme 1. Synthesis of the A and B Type Complexes

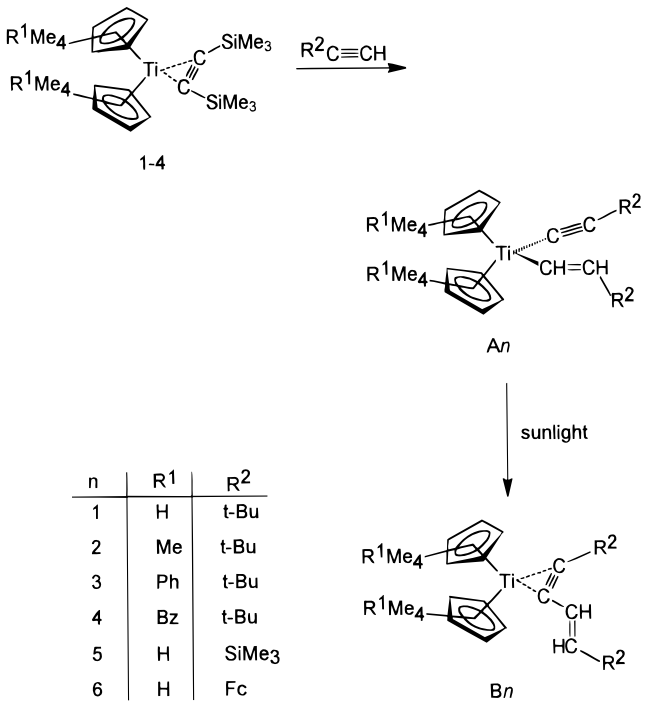

Crystal Structure of A1. In the solid state, complex **A1** exhibits a combined statistical and rotational disorder even at low temperature that lowers the precision of the structure determination (see Experimental Section). Hence, geometrical parameters describing the disordered hydrocarbyl ligands will not be discussed here in detail. Nevertheless, the chemical picture is unambiguous (Figure 1, Table 2) and verifies the structure assigned on the basis of spectral data. The molecular geometry of **A1** corresponds favorably to that of [(η^5-C_5Me_5)$_2$Ti(η-$C{\equiv}CPh$){η^1-(*E*)-$CH{=}CHPh$}].[9] The titanocene cyclopentadienyls are eclipsed with the *C*(Me)−*C*H edges at the hinge position, thus reflecting mimicked crystallographic C_2/σ symmetry.

(7) Horáček, M.; Císařová, I.; Karban, J.; Petrusová, L.; Mach, K. *J. Organomet. Chem.* **1999**, *577*, 103.

(8) (a) The stable, paramagnetic titanocene acetylide [(η^5-C_5Me_5)$_2$-Ti(η^1-C≡CMe)] was characterized: Luinstra, G. A.; ten Cate, L. C.; Heeres, H. J.; Pattiasina, J. W.; Meetsma, A.; Teuben, J. H. *Organometallics* **1991**, *10*, 3227. (b) An in situ generation of the cationic Ti(IV) titanocene monoacetylide [(η^5-C_5H_5)$_2$Ti(η^1-C≡CMe)] was also reported: Ahlers, R.; Erker, G.; Fröhlich, R. *J. Organomet. Chem.* **1998**, *571*, 83.

(9) Beckhaus, R.; Wagner, W.; Burlakov, V.; Baumann, W.; Peulecke, N.; Spannenberg, A.; Kempe, R.; Rosenthal, U. *Z. Anorg. Allg. Chem.* **1998**, *624*, 129.

(10) (a) Cohen, S. A.; Bercaw, J. E. *Organometallics* **1985**, *4*, 1006. (b) Burlakov, V. V.; Polyakov, A. V.; Yanovski, A. I.; Struchkov, Yu. T.; Shur, V. B.; Vol'pin, M. E.; Rosenthal, U.; Görls, H. *J. Organomet. Chem.* **1994**, *476*, 197. (c) Burlakov, V. V.; Rosenthal, U.; Beckhaus, R.; Polyakov, A. V.; Struchkov, Yu. T.; Oehme, G.; Shur, V. B.; Vol'pin, M. E. *Organomet. Chem. USSR* **1990**, *3*, 237. (d) Beckhaus, R.; Sang, J.; Oster, J.; Wagner, T. *J. Organomet. Chem.* **1994**, *484*, 179.

Table 1. Selected ^{13}C NMR Data (δ_C/ppm)[a] for A, B, and D Type Complexes

$[(\eta^5\text{-}C_5R^1Me_4)_2Ti(\eta^1\text{-}C{\equiv}CR^2)\{\eta^1\text{-}(E)\text{-}CH{=}CHR^2\}]$

compd	R^1	R^2	Ti−C≡*C*	Ti−*C*≡C	Ti−CH=*C*H	Ti−*C*H=CH
A1	C_5HMe_4	*t*-Bu	126.3	147.4	143.8	190.8
A2	C_5Me_5	*t*-Bu	124.2	149.4	142.5	193.2
A3	C_5PhMe_4	*t*-Bu	121.8	151.9	144.2	193.9
A4	C_5BzMe_4	*t*-Bu	124.6	150.1	143.1	193.5
A5	C_5HMe_4	$SiMe_3$	118.1	181.1	137.3	227.6
A6	C_5HMe_4	Fc	115.7	160.3	128.6	200.8

$[(\eta^5\text{-}C_5R^1Me_4)_2Ti\{\eta^2\text{-}(E)\text{-}R^2C{\equiv}CCH{=}CHR^2\}]$

compd	R^1	R^2	R^2−*C*≡C	R^2−C≡*C*	*C*H=CHR^2	CH=*C*HR^2
B1	C_5HMe_4	*t*-Bu	199.4	218.0	144.2	122.5
B2	C_5Me_5	*t*-Bu	203.9	218.6	144.0	123.1
B3	C_5PhMe_4	*t*-Bu	205.4	220.5	142.8	123.9
B4	C_5BzMe_4	*t*-Bu	204.7	219.6	144.7	123.2
B5	C_5HMe_4	$SiMe_3$	222.5	231.5	142.5	132.1
B6	C_5HMe_4	Fc	204.3	210.0	129.4	126.4

$[(\eta^5\text{-}C_5R^1Me_4)_2Ti\{\eta^2\text{-}(E)\text{-}R^2C{\equiv}CC(R^2){=}CH_2\}]$

compd	R^1	R^2	R^2−*C*≡C	R^2−*C*≡C	−*C*(R^2)=	=*C*H_2
D1	C_5HMe_4	$SiMe_3$	208.7	216.1	150.3	130.7
D2	C_5Me_5	$SiMe_3$	205.9	219.4	149.3	133.3
D3	C_5PhMe_4	$SiMe_3$	209.1	221.2	150.0	132.7

[a] In C_6D_6 at 298 K.

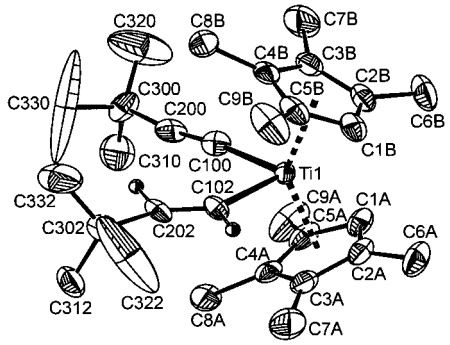

Figure 1. Molecular structure of **A1** with thermal ellipsoids drawn at the 30% probability level. For clarity, only one of the disordered hydrocarbyl ligands is shown and all methyl hydrogen atoms are omitted. Selected bond distances (Å) and angles (deg): Ti(1)−C(100) = 2.08(2), C(100)−C(200) = 1.26(2), C(200)−C(300) = 1.45(2), C(300)−C(320) = 1.46(2), C(300)−C(330) = 1.51(2), C(300)−C(310) = 1.52(2), Ti(1)−C(102) = 2.17(2), C(102)−C(202) = 1.27(2), C(202)−C(302) = 1.50(2), C(302)−C(312) = 1.51(2), C(302)−C(322) = 1.56(2), C(302)−C(332) = 1.46(2); C(100)−Ti(1)−C(102) = 91.3(3), Ti(1)−C(100)−C(200) = 173(1), C(100)−C(200)−C(300) = 171(2), Ti(1)−C(102)−C(202) = 129.3(8), C(102)−C(202)−C(302) = 138(1)°.

Crystal Structure of A6. The molecule of **A6** (Figure 2) consists of three metallocene units, whose bond lengths and angles are unexceptional (Table 2). Titanocene cyclopentadienyls adopt a conformation halfway between staggered and eclipsed, bearing the nonmethylated cyclopentadienyl carbons inclined toward each other to reduce the steric strain of the methyl groups on the rings. Cyclopentadienyls of both ferrocenyl groups are almost perfectly eclipsed, with dihedral angles of the least-squares cyclopentadienyl planes of 1.5 and 2.6° for the ethynyl- and ethenyl-substituted ferrocenyl group, respectively. The ferrocenyl groups are mutualy rotated at the dihedral angle subtended by the substituted cyclopentadienyls of 45.1°.

Undoubtedly, the most meaningful feature in the structure of **A6** is the geometry of ligation (Table 3). The titanium atom is pseudotetrahedrally coordinated, though, with angles markedly deviated from the value of the regular tetrahedron; C(1)−Ti−C(3) is more acute (92.1(3)°) because of unlike steric requirements of the cyclopentadienyl and both hydrocarbyl ligands. The Ti−C= and Ti−C≡ bond lengths of 2.127(7) and 2.102(7) Å, respectively, compare well with those observed for other titanium(IV) organometallics: $[(\eta^5\text{-}C_5Me_5)_2Ti(\eta^1\text{-}C{\equiv}CPh)(\eta^1\text{-}CH{=}CHPh)]$, 2.124(4) and 2.099(5) Å;[9] $[(\eta^5\text{-}C_5Me_5)_2Ti(\eta^1\text{-}CH{=}CH_2)(\eta^1\text{-}C{\equiv}CPh)]$, 2.14 and 2.10 Å (in the same order);[11] $[(\eta^5\text{-}C_5Me_5)_2TiF(\eta^1\text{-}CH{=}CH_2)]$, 2.098(6) Å (Ti−C=);[10d] $[(\eta^5\text{-}C_5H_5)_2Ti(\eta^1\text{-}C(Ph){=}CMe_2)Br_{0.5}\text{-}Cl_{0.5}]$, 2.234(4) Å (Ti−C=);[13] $[\{\eta^5\text{-}C_5(SiMe_3)H_4\}_2Ti(\eta^1\text{-}C{\equiv}C{-}C{\equiv}Fc)_2]$, 2.090(7) and 2.099(7) Å (Ti−C≡);[14] $[(\eta^5\text{-}C_5Me_5)_2Ti(OH)(\eta^1\text{-}C{\equiv}Ph)]$, 2.117(2) Å (Ti−C≡).[15] The fact that both Ti−C bond lengths are similar indicates that the η^1 ligands are simply σ-bonded with no significant π-bond contribution to the Ti−C bond such as Ti−C=C ↔ Ti⋯C⋯C and Ti−C≡C ↔ Ti=C=C.

The η^1-(*E*)-2-(ferrocenyl)ethenyl moiety possesses an arrangement typical for *trans*-disubstituted ethenes; the C(1)−C(2) bond length 1.312(9) Å is identical with the mean double-bond length observed in "organic" (*E*)-CC=CC fragments (1.31(1) Å; average value of 19 entries).[16] The Ti−C(1)−C(2) and C(1)−C(2)−C(11) angles are more opened due to different sizes of the substituents at the double bond, but no significant torsion occurs, as implied by the torsion angle Ti−C(1)−C(2)−C(11) of −170.7(5)°. Similarly, there is no deformation within the

(11) The structure determination is of low precision because of the presence of disordered η^5-C_5Me_5 ligands. Distances were retrieved from the Cambridge Crystallographic Data Centre[12] (CODEN: ZUXHEF). For the original reference see ref 23.

(12) Allen, F. H.; Kennard, O. *Chem. Design Automation News* **1993**, *8*, 1, 31.

(13) Cardin, C. J.; Cardin, D. J.; Morton-Blake, D. A.; Parge, H. E.; Roy, A. *J. Chem. Soc., Dalton Trans.* **1987**, 1641.

(14) Hayashi, Y.; Osawa, M.; Kobayashi, K.; Wakatsuki, Y. *J. Chem. Soc., Chem. Commun.* **1996**, 1617.

(15) Polse, J. L.; Andersen, R. A.; Bergman, R. G. *J. Am. Chem. Soc.* **1995**, *117*, 5393.

(16) Allen, F. H.; Kennard, O.; Watson, D. G.; Brammer, L.; Orpen, A. G.; Taylor, R. *J. Chem. Soc., Perkin Trans. 2* **1987**, S1.

Table 2. Selected Geometric Parameters of the Metallocene Units in A1, A6, B1, and D2 (in Å and deg)[a]

		A6				
compd	**A1** $(Me_4HC_5)_2Ti$	$(Me_4HC_5)_2Ti$	$(C_5H_5)Fe$ alkenic	$(C_5H_5)Fe$ alkynic	**B1** $(C_5Me_4H)_2Ti$	**D2** $(C_5Me_5)_2Ti$
CE−CE	3.897	3.887	3.301	3.290	3.917	3.982
M−CE	2.082[b]	2.096, 2.099	1.648, 1.653	1.649, 1.643	2.109, 2.107	2.111, 2.136
M−C(Cp)	2.348(2)−2.438(2)	2.357(6)−2.450(7)	av 2.04(2)	av 2.03(1)	2.347(6)−2.491(5)	2.412(2)−2.478(3)
av C−C(Cp)	1.410(5)	1.40(1)	1.40(2)	1.40(2)	1.402(8)	1.407(8)
av C(Cp)−C(Me)	1.498(4)	1.51(1)			1.504(6)	1.500(5)
∠(Cp,Cp)	47.8	48.3	1.5	2.6	44.9	40.2
CE−M−CE	138.9	135.9	177.8	177.9	136.6	139.3
av C−C−C(Cp)	108.0(5)	108(1)	108(1)	108(2)	108(1)	108.0(3)

[a] CE denotes the centroid of a cyclopentadienyl ring. [b] The M−CE distances are identical due to crystallographic symmetry.

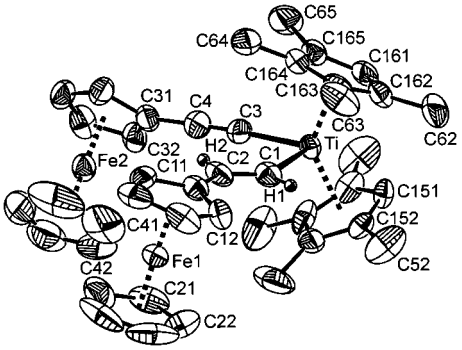

Figure 2. Molecular structure of **A6** (30% probability level, PLATON plot). Only alkenic hydrogen atoms are shown. For clarity, only pivot and adjacent carbon atoms of ferrocene rings are labeled and the numbering of the lower titanocene C_5HMe_4 ligand is analogous to that of the upper one.

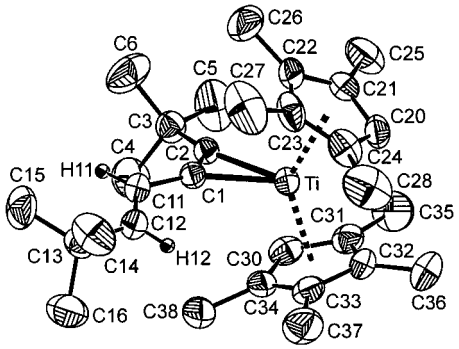

Figure 3. Molecular structure of **B1** (30% probability level, PLATON plot). All hydrogen atoms except those within the alkenyl moiety are omitted.

Table 3. Selected Bond Lengths (Å) and Bond Angles and Dihedral Angles (deg) for A6[a,b]

Ti−C(1)	2.127(7)	Ti−C(3)	2.102(7)
C(1)−C(2)	1.312(9)	C(3)−C(4)	1.174(8)
C(2)−C(11)	1.445(9)	C(4)−C(31)	1.445(9)
C(1)−Ti−C(3)	92.1(3)	Ti−C(3)−C(4)	172.3(6)
Ti−C(1)−C(2)	135.5(6)	C(3)−C(4)−C(31)	174.2(8)
C(1)−C(2)−C(11)	131.1(8)		
Ti−C(1)−C(2)−C(11)		−170.7(6)	
∠(TiC_2,Cp^1)	24.6(3)	∠(TiC_2,Cp^2)	23.8(4)
∠(TiC_2,Cp^3)	18.5(4)	∠(TiC_2,Cp^4)	50.9(3)

[a] Cf. Table 2. [b] Planes are defined as follows: TiC_2, Ti, C(3), and C(4); Cp^1, C(151)−C(155); Cp^2, C(161)−C(165); Cp^3, C(11)−C(15); Cp^4, C(31)−C(35).

η^1-bonded alkynyl ligand, as may be demonstrated by the bond lengths and angles within the Ti−C(3)−C(4)−C(31) fragment.

On exposure to direct sunlight, samples **A1**−**A6** (as C_6D_6 solutions in NMR tubes) change from orange-yellow to dark green or dark blue. Following the transformation by NMR indicated that the compounds were quantitatively converted into sole products (Scheme 1), all of them displaying similar features in their NMR spectra (Table 1). Large downfield shifts of the triple-bond carbon atoms into the region δ_C 190−250 are typical for triple-bonded carbons η^2-coordinated to a titanocene moiety.[10b,c,17] Furthermore, the presence of an uncoordinated (*E*)-CH═CH moiety was confirmed by the δ_C, δ_H and $^3J_{HH}$ values, indicating that the photo-induced reductive coupling of the hydrocarbyl ligands proceeds with no isomerization at the double bond. In UV−near-IR spectra, the long-wavelength electronic absorption band, observed in complexes **1**−**4** at 920 nm,[17a] is shifted for **B** type complexes to 720 nm, most likely as the consequence of conjugation of the multiple carbon−carbon bonds. The photolyses were repeated on a larger scale, and the products were isolated. Except for blue crystalline **B1**, whose crystal structure has been determined, other complexes could be isolated only in the form of dark blue-green (purple for **B6**) oils or waxy solids.

Crystal Structure of B1. The coordination geometry of **B1** (Figure 3, Table 4) resembles closely that of other titanacyclopropene-like titanocene−η^2-alkyne complexes. The most characteristic features are lengthening of the triple bond (1.304(6) Å) close to the value in cyclopropenes (1.29(2) Å, mean of 10 entries;[16] cf. the C−C bond lengths of 1.303 Å in both **1**[17a] and [(η^5-$C_5Me_4H)_2$Ti(η^2-FcC≡CSiMe_3)][17c]) and bending of the originally linear arrangement at the triple bond. Both Ti−C bond lengths are similar, thus pointing to a rather symmetric bonding of the alkyne to the titanocene framework with negligible torsion at the coordinated triple bond, as follows from the C(11)−C(1)−C(2)−C(3) torsion angle of −6(1)°. Similarly, the double bond exhibits no torsional distortion, adopting a typical *trans* double-bond geometry (1.314(7) Å vs mean value 1.31(1) Å for 19 (*E*)-CCH═CHC moieties).[16] The titanocene cyclopentadienyls are about halfway between staggered and eclipsed, with the nonmethylated carbon atoms mutually rotated similarly, as observed for the aforementioned [(η^5-$C_5Me_4H)_2$-Ti(η^2-FcC≡CSiMe_3)] complex.[17c] The dihedral angle

(17) (a) Varga, V.; Mach, K.; Polášek, M.; Sedmera, P.; Hiller, J.; Thewalt, U.; Troyanov, S. I. *J. Organomet. Chem.* **1996**, *506*, 241. (b) Rosenthal, U.; Görls, H.; Burlakov, V. V.; Shur, V. B.; Vol'pin, M. E. *J. Organomet. Chem.* **1992**, *426*, C53. (c) Štěpnička, P.; Gyepes, R.; Císařová, I.; Varga, V.; Polášek, M.; Horáček, M.; Mach, K. *Organometallics* **1999**, *18*, 627.

Table 4. Selected Bond Lengths (Å) and Bond Angles and Dihedral Angles (deg) for B1[a,b]

Ti−C(1)	2.068(5)	C(3)−C(4)	1.529(7)
Ti−C(2)	2.084(4)	C(3)−C(6)	1.538(7)
C(1)−C(2)	1.304(6)	C(12)−C(13)	1.516(6)
C(1)−C(11)	1.458(6)	C(13)−C(14)	1.525(6)
C(11)−C(12)	1.314(7)	C(13)−C(15)	1.518(6)
C(2)−C(3)	1.516(6)	C(13)−C(16)	1.523(6)
C(3)−C(5)	1.526(6)		

C(1)−Ti−C(2)	36.6(2)	C(4)−C(3)−C(5)	108.6(4)
Ti−C(1)−C(11)	150.6(4)	C(4)−C(3)−C(6)	107.5(4)
Ti−C(2)−C(3)	151.4(3)	C(5)−C(3)−C(6)	108.7(5)
C(2)−C(1)−C(11)	137.0(5)	C(12)−C(13)−C(14)	108.1(4)
C(1)−C(2)−C(3)	136.6(4)	C(12)−C(13)−C(15)	112.6(4)
C(1)−C(11)−C(12)	125.4(5)	C(12)−C(13)−C(16)	109.0(4)
C(11)−C(12)−C(13)	129.3(5)	C(14)−C(13)−C(15)	109.9(4)
C(2)−C(3)−C(4)	108.9(4)	C(14)−C(13)−C(16)	107.4(4)
C(2)−C(3)−C(5)	111.3(4)	C(15)−C(13)−C(16)	109.6(4)
C(2)−C(3)−C(6)	111.6(4)		

C(11)−C(1)−C(2)−C(3)	−6(1)
C(1)−C(11)−C(12)−C(13)	−176.0(5)

∠(TiC$_2$,Cp^1)	24.6(4)	∠(TiC$_2$,Cp^2)	21.0(4)

[a] Cf. Table 2. [b] Planes are defined as follows: TiC$_2$: Ti, C(1) and C(2); Cp^1: C(20)−C(24); Cp^2: C(30)−C(34).

subtended by the least-squares planes of the cyclopentadienyl rings (44.9°) in **B1** is about the average of those in **1** (50.0°) and **2** (41.1°),[18] apparently because only one of the CH groups on the η^5-C_5Me_4H ligands is placed at the hinge position. The CH group of the other η^5-C_5Me_4H ligand is directed toward the *t*-Bu group of the cordinated alkyne (see Figure 3). In the structure of **1**, two bulky $SiMe_3$ groups at the coordinated triple bond constrain both CH groups to reside at the hinge position. A significantly shorter C(2)−C(3) distance in **B1** (1.516(6) Å) compared to the ≡C−Si distance in **1** (1.853(3) Å;[17a] cf. the C(1)−Si(1) distance 1.855(2) Å in **D2** below or 1.859(3) Å (average) in **2**[10b]) boosts steric demands of the coordinated alkyne and, hence, results in an opening of the titanocene framework and also increases strain of the substituents on its cyclopentadienyls.

As the **B** type complexes cannot obviously participate in the catalytic cycle yielding HTT dimers, we set out to prove the stability of the titanocene−HTT dimer complexes which have to occur as intermediates in the catalytic cycle. The reduction of the appropriate titanocene dichlorides by magnesium in THF in the presence of $Me_3SiC{\equiv}CC(SiMe_3){=}CH_2$ afforded compounds **D1**−**D3** in nearly quantitative yields (Scheme 2). Their NMR spectra indicated η^2 coordination of the triple bond with the double bond kept intact (Table 1). The fact that the compounds display an absorption band at 925 nm, i.e., in the same region as the titanocene−BTMSE complexes **1**−**4**, may indicate that the conjugation of unsaturated bonds in HTT dimer is interrupted.

Crystal Structure of D2. The parameters of the molecular structure of **D2** determined by single-crystal X-ray diffraction (Tables 2 and 5) confirmed that the HTT dimer is bonded to the titanocene framework as a simple η^2-alkyne (Figure 4). The C−C bond length of the coordinated alkyne corresponds nicely to the values reported for [(η^5-$C_5Me_5)_2$Ti(η^2-$R^1C{\equiv}CR^2$)] complexes (R^1/R^2: $(SiMe_3)_2$, 1.309(4) Å; Ph/$SiMe_3$, 1.308(3)Å;[9b] Fc/Ph, 1.312(5) Å[17c]) and the (η^5-$C_5Me_4H)_2$Ti complexes **B1** and

(18) Varga, V.; Hiller, J.; Gyepes, R.; Polášek, M.; Sedmera, P.; Thewalt, U.; Mach, K. *J. Organomet. Chem.* **1997**, *538*, 63.

Scheme 2. Synthesis of the D Type Complexes

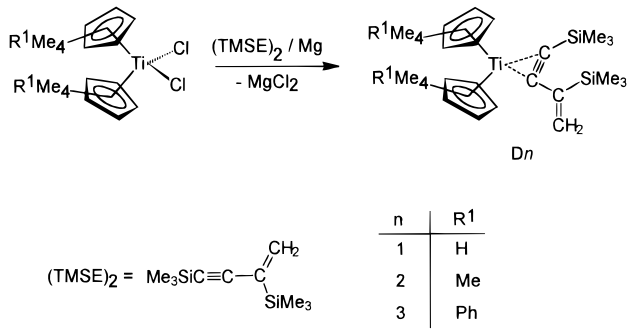

n	R^1
1	H
2	Me
3	Ph

Table 5. Selected Bond Lengths (Å) and Bond Angles and Dihedral Angles (deg) for D2[a,b]

Ti−C(1)	2.163(2)	Si(1)−C(6)	1.885(3)
Ti−C(2)	2.102(2)	Si(1)−C(7)	1.870(3)
C(1)−C(2)	1.300(3)	C(3)−Si(2)	1.887(2)
C(2)−C(3)	1.467(3)	Si(2)−C(8)	1.849(3)
C(3)−C(4)	1.317(4)	Si(2)−C(9)	1.858(4)
C(1)−Si(1)	1.855(2)	Si(2)−C(10)	1.864(3)
Si(1)−C(5)	1.873(3)		

C(2)−Ti−C(1)	35.44(8)	C(1)−Si(1)−C(7)	111.0(1)
Ti−C(1)−Si(1)	141.6(1)	C(5)−Si(1)−C(6)	105.4(2)
Ti−C(2)−C(3)	140.2(2)	C(5)−Si(1)−C(7)	105.4(2)
Si(1)−C(1)−C(2)	148.6(2)	C(6)−Si(1)−C(7)	107.3(2)
C(1)−C(2)−C(3)	145.0(2)	C(3)−Si(2)−C(8)	111.0(1)
C(2)−C(3)−C(4)	119.0(2)	C(3)−Si(2)−C(9)	107.8(1)
C(2)−C(3)−Si(2)	123.0(2)	C(3)−Si(2)−C(10)	110.3(2)
C(4)−C(3)−Si(2)	118.0(2)	C(8)−Si(2)−C(9)	112.5(2)
C(1)−Si(1)−C(5)	114.7(2)	C(8)−Si(2)−C(10)	107.4(2)
C(1)−Si(1)−C(6)	112.6(1)	C(9)−Si(2)−C(10)	107.8(2)

Si(1)−C(1)−C(2)−C(3)	−1.2(6)
C(1)−C(2)−C(3)−Si(2)	−8.8(4)
C(1)−C(2)−C(3)−C(4)	173.8(3)

∠(TiC$_2$,Cp^1)	19.7(2)	∠(TiC$_2$,Cp^2)	20.6(2)

[a] Cf. Table 2. [b] Planes are defined as follows: TiC$_2$, Ti, C(1) and C(2); Cp^1, C(11)−C(15); Cp^2, C(21)−C(25).

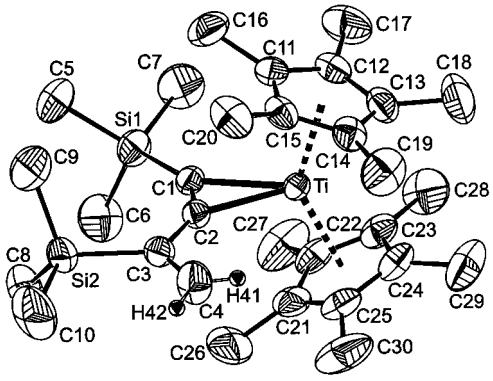

Figure 4. Molecular structure of **D2** (30% probability level, PLATON plot). Hydrogen atoms, except those of the terminal methylene group, are omitted for clarity.

1 mentioned above. The dihedral angle of the cyclopentadienyl planes in **D2** (40.2°) is similar to that of [(η^5-$C_5Me_5)_2$Ti(η^2-PhC≡CSiMe_3)] (40.6°), and very slightly lower than that in **2** (41.1°).[9b] The arrangement of the SiC(=C)C≡CSi moiety deviates only marginally from an overall planarity, as indicated by torsion angles. The C=CH_2 moiety is directed out of the titanocene framework, and bond lengths and angles within it appear conventional when compared to the values for "organic" $C_2C{=}CH_2$ units (C=C = 1.32(1) Å, arithmetic mean of 77 entries).[16] In keeping with the interruption of

Scheme 3. Chemistry Underlying the HTT Dimerization of Terminal Alkynes Catalyzed by Titanocene−BTMSE Complexes (Cp″ = η^5-C_5Me_4H, η^5-C_5Me_5)

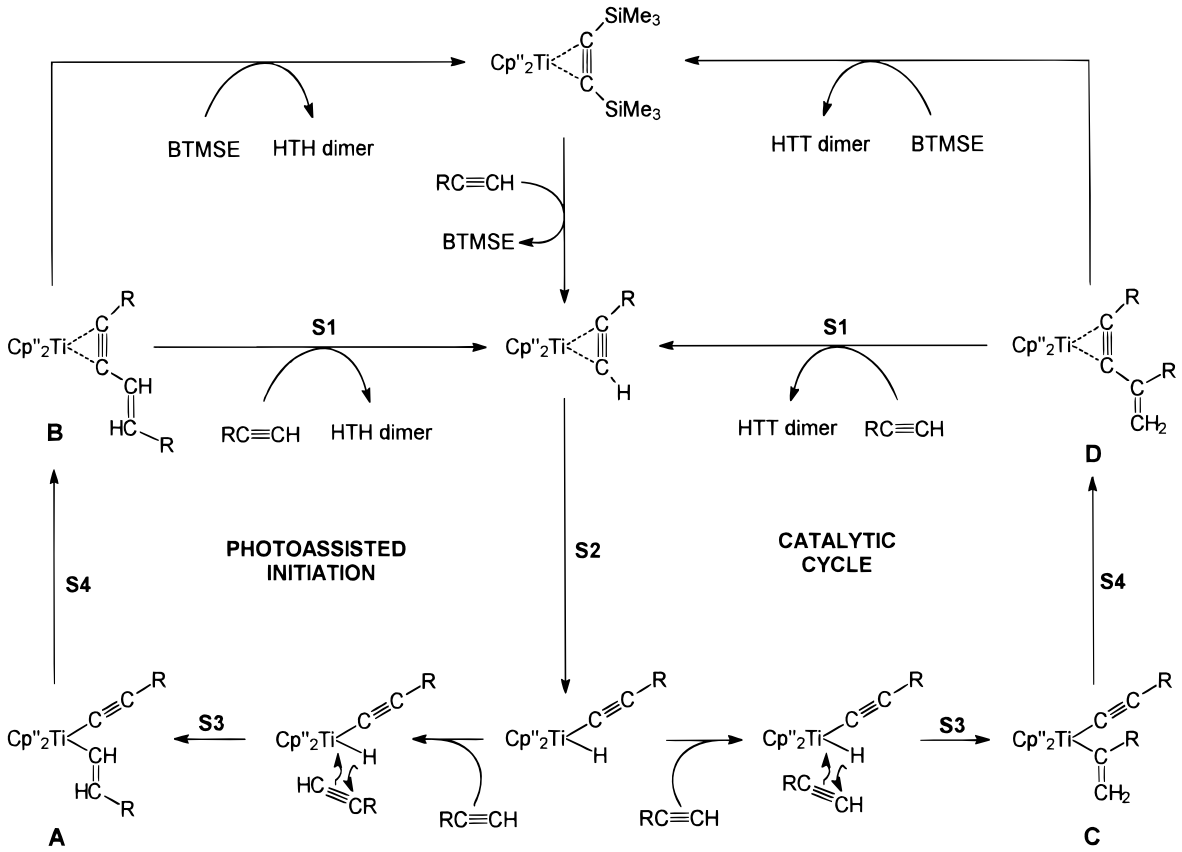

conjugation deduced from UV−near-IR spectra, the C(2)−C(3) distance (1.467(3) Å) is slightly longer than the mean C=*C*−*C*≡C bond length observed in noncoordinated enynes (1.43(1) Å; 11 entries).[16]

Different results were obtained using the HTT dimer $(TBUE)_2$ as the alkyne, since a similar reduction of a *t*-BuCC≡C(*t*-Bu)=CH_2/[(η^5-$C_5Me_5)_2TiCl_2$] mixture afforded a purple solution which contained the paramagnetic complex [(η^1:η^5-$C_5Me_4CH_2$)(η^5-C_5Me_5)Ti],[19] instead of the desired compound [(η^5-$C_5Me_5)_2$Ti{η^2-*t*-BuCC≡C(*t*-Bu)=CH_2}]. This may well reflect the fact that decamethyltitanocene-based catalysts do not dimerize TBUE as the only terminal alkyne. Under similar conditions, the less sterically crowded[20] complex [(η^5-$C_5Me_4H)_2$Ti-{η^2-(*t*-Bu)CC≡C(*t*-Bu)=CH_2}] was formed according to NMR spectra; however, it was accompanied by another product whose nature remains yet unclear.

Reactivity of Complexes 1 and 2, and Compounds of the A, B, and D Types Derived Thereof, toward TBUE and TMSE. It has been shown previously that (η^5-$C_5Me_5)_2$Ti-based complexes catalyze the HTT dimerization of all nonpolar 1-alkynes except TBUE,[1a,5,6] whereas (η^5-$C_5Me_4H)_2$Ti-derived complexes accomplish this catalysis for TBUE only.[7] The present results demonstrate in addition that both complexes **1** and **2** react in the dark with an excess of terminal alkynes to give **A** type complexes (Scheme 3, left), whereas upon exposure to sunlight, the complexes **1** and **2** induce a rapid HTT dimerization of TBUE and TMSE, respectively. Although the experiments with these highly air- and moisture-sensitive materials performed in all-sealed optical cells did not enable us to follow the kinetics of the dimerization rigorously under constant concentration of the alkynes, it is obvious that reaction rates as high as 5×10^2 turnovers h^{-1} were achieved, much higher than dimerization rates observed for **2** in diffuse daylight.[6] The assumption that this photoinduced catalysis is closely connected with the photoinduced reductive coupling of the carbyl ligands in **A** type complexes, affording complexes with HTH dimers η^2-coordinated through their triple bond (type **B**), was proved by the observation that complexes **B1** and **B2** effectively dimerize TBUE and TMSE, respectively, in the dark.

Furthermore, titanocene complexes with the HTT dimer $(TMSE)_2$ were prepared (type **D**), and its decamethyltitanocene representative **D2** showed a high catalytic activity toward the HTT dimerization of TMSE in the dark. The high reactivity of **D2** was also demonstrated by its facile conversion into **A2** by addition of TBUE (note that TBUE does not dimerize on (η^5-$C_5Me_5)_2$Ti catalysts). On the other hand, the reluctance of the HTT dimer $(TBUE)_2$ to form a **D** type complex with decamethyltitanocene accounts very likely for the inactivity of decamethyltitanocene complexes in the HTT dimerization of TBUE. Complexes **B1** and **D2** also

(19) (a) Fischer, J. M.; Piers, W. E.; Young, V. G., Jr. *Organometallics* **1996**, *15*, 2410. (b) Bercaw, J. E.; Brintzinger, H. H. *J. Am. Chem. Soc.* **1971**, *93*, 2048. (c) Bercaw, J. E. *J. Am. Chem. Soc.* **1974**, *96*, 5087. (d) Luinstra, G. A.; Teuben, J. H. *J. Am. Chem. Soc.* **1992**, *114*, 3361.

(20) Dihedral angles between the least-squares planes of the cyclopentadienyl rings in the [(η^5-$C_5Me_4H)_2TiL_n$] complexes (L_n = Cl, Cl_2, and BTMSA) are ca. 9° larger than those in their [(η^5-$C_5Me_5)_2TiL_n$] analogues.[18]

underwent a smooth ligand exchange with BTMSE to give **1** and **2**, respectively, and noncoordinated $(TMSE)_2$.

Implications for the Catalysis of Dimerization and Related Reactions. Regarding the above results, the catalytic cycle suggested previously[6] is essentially valid; however, it requires initiation by light. The **A** type complexes formed in the dark by a formal displacement of the coordinated BTMSE with two molecules of a terminal alkyne have to be first photoconverted to **B** type complexes (Scheme 3, left) which then trigger the catalytic cycle (Scheme 3, right). Complexes **B** undergo easily a displacement of the η^2-coordinated HTH dimer with terminal alkynes, thus affording the plausible intermediates $[(Cp'')_2Ti(\eta^2\text{-}RC{\equiv}CH)]$ and $[(Cp'')_2Ti(H)(\eta^1\text{-}C{\equiv}CR)]$ ($Cp'' = \eta^5\text{-}C_5Me_4H$, $\eta^5\text{-}C_5Me_5$) (steps **S1** and **S2**). The involvement of titanocene−acetylide−hydride in the mechanism is corroborated by the reaction of **2** with MeOH, yielding the hydride $[(\eta^5\text{-}C_5Me_5)_2Ti(H)(OMe)]$, though it did not exert any reaction with 1-hexyne,[9] very likely due to the formation of a strong Ti−O bond. Although the following step, i.e., regioselective insertion of the second molecule of 1-alkyne into the Ti−H bond (step **S3**, tail-on insertion) providing **C** type complexes, lacks direct experimental evidence, it leads, after reductive coupling of the carbyl ligands (step **S4**), to the characterized but rather reactive **D** type complexes. Then, the cycle is reinitiated by an exchange of the coordinated HTT dimer for the terminal alkyne (step **S1**)—but started anew, it proceeds with no participation of **A** and **B** type complexes (Scheme 3, right).

A conversion of the titanocene−acetylide−hydride intermediate into the titanocene−vinylidene species proposed by Beckhaus et al.[9] can be inserted in the reaction mechanism as an alternative to step **S2**, since such rearrangements are well-documented for late-transition-metal[21] and even decamethyltitanocene complexes.[22] It has been shown that the vinylidene complex $[(\eta^5\text{-}C_5Me_5)_2Ti{=}C{=}CH_2]$ reacts with 1-alkynes to afford η^1-vinyl η^1-alkynyl compounds.[23] Nonetheless, the vinylidene intermediate cannot furnish **C** type complexes, which are the apparent precursors of the **D** type compounds. The **D** type complexes undoubtedly belong in the catalytic cycle, since they efficiently initiate the HTT dimerization in the dark.

The formation of the **A** type complexes proceeds analogously, differing only in an opposite insertion (head-on) of the 1-alkyne into the Ti−H bond. The origin of such a reaction dichotomy remains unknown.[24] In a comparison of the reactivity of **A** and **C** type complexes, the former are less reactive, requiring a photoexcitation to rearrange into the complexes with coupled carbyl ligands. Taking into account that the substituent in the alkenic part of the **C** type complexes is separated from the titanocene framework by only a C_1 spacer whereas **A** type complexes possess a C_2 spacer that reduces the steric strain, the different reactivities are in full accordance with the general observation that bulky substituents facilitate reductive elimination. The unfavorable reductive coupling **A** → **B** becomes possible on irradiation, since photoexcitation lowers electron density at the titanium atom through its transfer into diffuse orbitals with higher principal quantum number or ligand-based orbitals (MLCT) and, in this way, enhances susceptibility of the titanocene complex to undergo reductive elimination.[25] Similar reductive couplings of vinyl groups to 1,3-butadiene[22] and two alkynyl groups to butadiynes are known for permethyltitanocene and permethylzirconocene complexes.[26]

A facile exchange of the coordinated alkyne dimers for BTMSE in both **B** and **D** type complexes may represent one of the deactivation pathways,[27] which converts ultimately in the absence of light all titanium complexes into the **A** type complexes. However, in light, the catalytic cycle is easily resumed via triggering by a **B** type complex. Although the leaving BTMSE or HTH dimer may play some role in the control of the reaction pathway, it can hardly account for the high selectivity of the HTT dimer formation. The photoinitiated mechanism should produce at least one molecule of HTH dimer per one molecule of the BTMSE complex and another molecule for each photoreinitiation step. With total turnover numbers of about 1×10^3,[6,7] the presence of less than 1% of HTH in HTT dimers falls below the precision of GC-MS and NMR analysis.

Although the reactions connected to the photoassisted catalytic HTT dimerization of terminal alkynes seem to be reliably clarified, we anticipate that our present knowledge does not allow us to prove unequivocally the role of the plausible **C** type intermediates. Further studies on the stability of the **C** type complexes and the rate of their conversion into the corresponding **D** type complexes as well as the stability of **D** type complexes with $(TBUE)_2$ are in progress.

Experimental Section

General Considerations. All manipulations with titanium complexes and the dimerization experiments were carried out on a high-vacuum−argon line operated by means of nongreased glass-to-metal sealed valves (Hoke) in all-sealed glass devices equipped with breakable seals, sealed quartz cuvettes, and ESR sample tubes. Glass-to-glass sealed NMR sample tubes were filled with C_6D_6 solutions using evacuated all-glass devices and were sealed off by flame. The adjustment of single crystals into Lindemann glass capillaries for X-ray analyses and the preparations of KBr pellets for IR measurements were made in a glovebox under purified nitrogen (mBraun, O_2 and

(21) Bruce, M. I. *Chem. Rev.* **1991**, *91*, 197.

(22) Beckhaus, R. In *Metallocenes*; Togni, A., Halterman, R. L., Eds.; Wiley-VCH: Weinheim, Germany, 1998; Vol. 1, Chapter 4.4, pp 175−210.

(23) Beckhaus, R.; Sang, J.; Wagner, T.; Ganter, B. *Organometallics* **1996**, *15*, 1176.

(24) Similarly to other hydrometalations with neutral hydrides, the insertion step is a *cis* addition (at least step **S3**) but, surprisingly, it lacks the regioselectivity encountered in other hydrometalations; the following references may serve as leading examples. (a) Addition of $[(\eta^5\text{-}C_5H_5)Zr(H)Cl]$ and other transition-metal−H bonds: Labinger, J. A. In *Comprehensive Organic Synthesis*; Trost, B. M., Ed.; Pergamon Press: Oxford, U.K., 1991; Vol. 8, pp 667−702. (b) R_2AlH: Eisch, J. J. In *Comprehensive Organic Synthesis*; Trost, B. M., Ed.; Pergamon Press: Oxford, U.K., 1991; Vol. 8, pp 733−753. (c) $[RuH(Cl)(CO)(PPh_3)_2]$: Hill, A. F. In *Comprehensive Organometallic Chemistry II*; Abel, E. W., Stone, F. G. A., Wilkinson, G., Eds.; Pergamon Press: Oxford, U.K., 1995; Vol. 7, pp 399−406.

(25) See, for instance: (a) Collman, J. P.; Hegedus, L. S. *Principles and Applications of Organotransition Metal Chemistry*; University Science Books: Mill Valley, CA, 1980; pp 232−251. (b) Crabtree, R. H. *The Organometallic Chemistry of the Transition Metals*, 2nd ed.; Wiley: New York, 1994; pp 151−158.

(26) Pellny, P.-M.; Kirchbauer, F. G.; Burlakov, V. V.; Baumann, W.; Spannenberg, A.; Rosenthal, U. *J. Am. Chem. Soc.* **1999**, *121*, 8313.

(27) One of the reviewers suggested that the deactivation may proceed as a side reaction of the alkynyl−hydrido intermediate with the alkyne: $[(\eta^5\text{-}C_5Me_5)_2Ti(H)(C{\equiv}CR)] + RC{\equiv}CH \rightarrow [(\eta^5\text{-}C_5Me_5)_2Ti(\eta^1\text{-}C{\equiv}CR)_2] + H_2$.[26]

H_2O concentrations lower than 2.0 ppm). ^1H (399.95 MHz) and ^{13}C (100.58 MHz) NMR spectra were measured on a Varian UNITY Inova 400 spectrometer in C_6D_6 solutions at 298(1) K. Chemical shifts (δ/ppm) are referenced to the solvent signal (δ_H 7.15, δ_C 128.0). ^{29}Si (79.46 MHz) NMR spectra were recorded by the standard DEPT technique; ^{29}Si chemical shifts are given relative to external tetramethylsilane (δ_{Si} 0) and assigned by comparison with δ_{Si} values of related compounds.[28] Mass spectra were measured on a VG 7070E spectrometer at 75 eV using a direct inlet probe (samples in sealed capillaries were opened and inserted into the probe under argon). UV−near-IR spectra were measured in the range of 270−2000 nm on a Varian Cary 17D spectrometer using all-sealed quartz cuvettes (Hellma). Infrared spectra in KBr pellets or as hexane solutions were obtained on a Specord IR-75 (Carl Zeiss, Jena, Germany) spectrometer. GC analyses were performed on a CHROM 5 gas chromatograph (Laboratory Instruments, Prague, Czech Republic) equipped with 10% SE-30 on a Chromaton N-AW-DMCS column. GC-MS analyses were carried out on a Hewlett-Packard gas chromatograph (5890 series II; capillary column SPB-1 (Supelco)) interfaced to a mass spectrometric detector (5791 A). Melting points were determined for samples in N_2-filled sealed capillaries on a Kofler apparatus and are uncorrected.

Hexane, toluene, and tetrahydrofuran (THF) were dried by refluxing over $LiAlH_4$ under an argon atmosphere, degassed, and stored as solutions of green dimeric titanocene [(μ-η^5:η^5-$C_{10}H_8$){(η^5-C_5H_5)Ti(μ-H)}$_2$][29] on a vacuum line. Likewise, C_6D_6 was degassed and stored as a solution of green dimeric titanocene on a vacuum line. *tert*-Butylethyne (TBUE) and (trimethylsilyl)ethyne (TMSE) (Aldrich) were degassed and distilled onto dimeric titanocene under vacuum. After the solutions had turned green-brown (ca. 3 h), the alkynes were distilled under vacuum into storage vessels. Similarly, TBUE was further treated with solid [{(η^5-C_5Me_5)$_2$Ti(μ-H)$_2$}$_2$Mg] complex[30] to remove traces of *tert*-butyl alcohol. Ferrocenylethyne[31] was carefully degassed under vacuum and dissolved in toluene. The complexes [(η^5-C_5Me_4R)$_2$TiCl$_2$] (R = H, Me,[32] Ph,[33] Bz[34]) were prepared by the literature procedures.

All [(η^5-C_5Me_4R)$_2$Ti(η^2-BTMSE)] complexes were prepared by the reduction of the corresponding titanocene dichlorides [(η^2-C_5Me_4R)$_2$TiCl$_2$] in THF using an excess of Mg and BTMSE.[10b,c,17a] The compounds [(η^5-C_5Me_4R)$_2$Ti(η^2-BTMSE)], where R = H (**1**) and Me (**2**), were identical with those previously described.[17a]

[(η^5-C_5Me_4Ph)$_2$Ti(η^2-BTMSE)] (3). Mp: 157 °C. ^1H NMR (C_6D_6): δ −0.06 (s, 9 H, *Me*$_3$Si), 1.83, 1.98 (2 × s, 6 H, C_5*Me*$_4$Ph), 6.25−6.32 (apparent bd, 2 H, *Ph*), 6.91−7.40 (m, 3 H, *Ph*). $^{13}C\{^1H\}$ NMR (C_6D_6): δ 3.8 (*Me*$_3$Si), 13.4, 14.7 (2 × C_5*Me*$_4$Ph), 123.1, 125.2 (C_5Me_4Ph, *C*Me), 126.0, 129.2 (Ph, *C*H), 126.6, 137.8 (Ph, C_{ipso} Ph, and C_5Me_4Ph, *C*Ph), 251.0 (η^2-*C*≡*C*). One of the *C*H(Ph) signals is overlapped by the solvent resonance. ^{29}Si NMR (C_6D_6): δ −15.8 (Me$_3$*Si*). EI MS (direct inlet, 120 °C): M$^{\bullet+}$ not observed; ions due to BTMSE (*m*/*z* 155, 97, 73, 70, 45) and titanocene (*m*/*z* 442 [(C_5Me_4Ph)$_2$Ti]$^{\bullet+}$ and *m*/*z* 221 [(C_5Me_4Ph)$_2$Ti]$^{2+}$) indicate that the complex dissociates on heating in the probe or during electron impact. IR (KBr, cm^{-1}): 3043 (m,b), 2948 (s,b), 2889 (s,b), 2850 (sh), 1597 (s), 1557 (s), 1503 (m), 1436 (m,b), 1371 (m), 1245 (vs), 1239 (vs), 1071 (m), 847 (vs,b), 827 (sh), 755 (vs), 698 (vs), 653 (m), 444 (m). UV−near-IR (hexane, nm): 915.

[(η^5-C_5Me_4Bz)$_2$Ti(η^2-BTMSE)] (4). ^1H NMR (C_6D_6): δ 0.03 (s, 9 H, Si*Me*$_3$), 1.61, 1.76 (2 × s, 6 H, C_5*Me*$_4$Bz); 3.69 (s, 2 H, PhC*H*$_2$), 7.11−7.53 (m, 5 H, *Ph*). $^{13}C\{^1H\}$ NMR (C_6D_6): δ 4.5 (Si*Me*$_3$), 12.4, 13.1 (C_5*Me*$_4$Bz); 34.2 (PhCH$_2$), 121.8, 122.9 (C_5-Me$_4$Bz, *C*Me); 126.1 (Ph, C_{ipso}), 126.2 (Ph, *C*H$_p$), 128.6, 128.9 (Ph, *C*H$_{o,m}$); 142.2 (C_5Me_4Bz, *C*CH$_2$), 249.1 (η^2-*C*≡*C*). EI MS (direct inlet, 120 °C): M$^{\bullet+}$ not observed; the ion of titanocene [(C_5Me_4Bz)$_2$Ti]$^{\bullet+}$ (*m*/*z* 470) during the course of measurement is replaced by the signal of the allyl diene compound [(C_5Me_4-Bz)$_2$Ti − 2H]$^+$ (*m*/*z* 468); ions due to BTMSE (*m*/*z* 155, 97, 73) and bis(trimethylsilylethene) (*m*/*z* 157) are also observed, varying in intensity. IR (KBr, cm^{-1}): 1595. UV−near-IR (hexane, nm): 920.

Reaction of the Complexes [(η^5-C_5Me_4R)$_2$Ti(η^2-BTMSE)] (R = H, Me, Ph, Bz) with TBUE, TMSE, and FCE. Only a representative synthesis of **A1** is given in detail, since the other experiments with TBUE and TMSE were performed similarly. The procedures differ only in the reaction time necessary to convert all of the BTMSE complex.

[(η^5-C_5Me_4H)$_2$Ti{η^1-(*E*)-CH=CHCMe$_3$}(η^1-C≡CCMe$_3$)] (A1). Purified TBUE (1.0 mL, 8 mmol) was condensed on a vacuum line into the solution of **1** (0.46 g, 1.0 mmol) in hexane (20 mL). The resulting yellow solution was heated in the dark to 60 °C in a sealed ampule equipped with an all-sealed quartz cell (d = 1.0 mm), while conversion was monitored by following the intensity decrease of the absorption bands at 920 and 1530 nm, which are due to complex **1** and TBUE (2 × ν(≡CH)), respectively. The absorption band of the starting titanocene complex disappeared after about 6 h at 60 °C in the dark, and approximately 2 mmol of TBUE was consumed within this period. No further consumption of TBUE was observed thereafter. All volatiles were distilled under vacuum into a trap cooled by liquid nitrogen overnight, and the remaining yellow solid was dissolved in a minimum amount of hexane (2 mL). After it was cooled overnight to −18 °C, this solution afforded large yellow crystals. The mother liquor was separated, and the crystallization was repeated. Despite the fact that the conversion was apparently quantitative, the yield of yellow crystals of **A1** was only 0.34 g (75%) due to their high solubility in hexane. In all the experiments, the volatiles were controlled for the presence of the liberated BTMSE and the content of HTT dimer. The molar ratio HTT dimer/BTMSE varied from 0.2 to 2.0 when the reaction was carried out in the dark. Data for **A1** are as follows. ^1H NMR (C_6D_6): δ 1.09, 1.24 (2 × s, 9 H, *Me*$_3$C); 1.60, 1.77, 1.96, 2.22 (4 × s, 6 H, C_5*Me*$_4$H); 4.74 (s, 2 H, C_5Me_4*H*), 4.90 (d, 1 H, $^3J_{HH}$ = 17.0 Hz, TiCH=C*H*), 5.19 (d, 1 H, $^3J_{HH}$ = 17.0 Hz, TiC*H*=CH). $^{13}C\{^1H\}$ NMR (C_6D_6): δ 13.2, 14.1 (2 C), 15.0 (C_5*Me*$_4$H), 28.1 (Me$_3$*C*), 30.4, 31.8 (*Me*$_3$C), 35.3 (Me$_3$*C*), 108.8 (C_5Me_4H, *C*H), 119.8, 120.1 (C_5Me_4H, *C*Me), 122.7 (TiC≡*C*), 126.3, 126.8 (C_5Me_4H, *C*Me), 143.8 (TiCH=*C*H), 147.4 (Ti*C*≡C), 190.8 (Ti*C*H=CH). EI-MS (direct inlet, 70 eV, 90 °C): *m*/*z* (relative abundance) 454 (*M*$^{\bullet+}$; 1), 372 ([*M* − TBUE]$^+$; 14), 292 (10), 291 (26), 290 ([*M* − 2 TBUE]$^+$; 100), 289 (25), 288 (17), 168 (7), 167 (12), 166 (9), 164 (15), 149 (9), 121 (8), 107 (10), 105 (8), 91 (10), 77 (7), 57 (7), 41 (15). IR (KBr, cm^{-1}): 2940 (vs), 2900 (vs,b), 2847 (vs), 2076 (s), 1500 (m), 1477 (s), 1466 (s), 1451 (vs), 1433 (s), 1377 (s), 1365 (s), 1356 (s), 1245 (vs), 1200 (s), 1148 (m), 1113 (m), 1032 (sh), 1022 (s), 1002 (s), 980 (m), 894 (m), 832 (vs), 821 (vs), 797 (m), 731 (s), 697 (m), 606 (m), 506 (m), 468 (s), 458 (vs), 420 (m). UV−near-IR (hexane, nm): 410 > 465 (sh). Anal. Calcd for $C_{30}H_{46}Ti$: C, 79.27; H, 10.20. Found: C, 79.30; H, 10.22.

[(η^5-C_5Me_5)$_2$Ti{η^1-(*E*)-CH=CHCMe$_3$}(η^1-C≡CCMe$_3$)] (A2). As indicated by the decay of the absorption band of **2** at 916 nm, the reaction was completed after 10 h at 60 °C. Approximately 2 mmol of TBUE was consumed, and no further consumption was observed after that time. Volatiles were evaporated under vacuum, leaving a yellow residue, which was

(28) δ_{Si}: BTMSE −19.2, [(η^5-Me$_n$C$_5$H$_{5-n}$)$_2$Ti(η^2-BTMSE)]; −15.7 for n = 5, −17.2 for n = 4 under the same conditions.

(29) Antropiusová, H.; Dosedlová, A.; Hanuš, V.; Mach, K. *Transition Met. Chem.* **1981**, *6*, 90.

(30) Troyanov, S. I.; Varga, V.; Mach, K. *J. Chem. Soc., Chem. Commun.* **1993**, 1174.

(31) (a) Rosenblum, M.; Brawn, N.; Papenmeier, J.; Applebaum, M. *J. Organomet. Chem.* **1966**, *6*, 173. (b) Rosenblum, M.; Brawn, N. M.; Ciappenelli, D.; Tancrede, J. *J. Organomet. Chem.* **1970**, *24*, 469.

(32) Mach, K.; Antropiusová, H.; Varga, V.; Poláček, J. *J. Organomet. Chem.* **1987**, *333*, 205.

(33) Horáček, M.; Poláček, M.; Kupfer, V.; Thewalt, U.; Mach, K. *Collect. Czech. Chem. Commun.* **1999**, *64*, 61.

(34) Langmaier, J.; Samec, Z.; Varga, V.; Horáček, M.; Mach, K. *J. Organomet. Chem.* **1999**, *579*, 348.

dissolved in the minimum amount of hexane and cooled to give **A2** as an yellow waxy solid, yield 0.42 g (87%). Volatiles contained HTT dimer and BTMSE in the molar ratio ca. 2:1. ^{1}H NMR (C_6D_6): δ 1.11, 1.28 (2 × s, 9 H, *Me*$_3$C), 1.82 (s, 30 H, C_5*Me*$_5$), 4.77 (d, 1 H, $^3J_{HH}$ = 16.6 Hz, TiCH=C*H*), 5.03 (d, 1 H, $^3J_{HH}$ = 16.6 Hz, TiC*H*=CH). ^{13}C{^{1}H} NMR (C_6D_6): δ 12.9 (C_5*Me*$_5$), 28.2 (Me$_3$*C*), 30.4, 31.9 (*Me*$_3$C), 35.4 (Me$_3$*C*), 121.1 (*C*$_5$Me$_5$), 124.2 (TiC≡*C*), 142.5 (TiCH=*C*H), 149.4 (Ti*C*≡C), 193.2 (Ti*C*H=CH). UV−near-IR (hexane, nm): 405 (sh) > 480 (sh).

[(η^5-C_5Me_4Ph)$_2$Ti{η^1-(*E*)-CH=CHCMe$_3$}(η^1-C≡CCMe$_3$)] (A3). The absorption band of **3** at 915 nm disappeared after 4 h at 60 °C. The consumption of TBUE was approximately 2 equiv. **A3** was formed as an orange waxy solid, yield 0.61 g (ca. 100%). ^{1}H NMR (C_6D_6): δ 1.10, 1.30 (2 × s, 9 H, *Me*$_3$C), 1.70, 1.91, 2.00, 2.03 (4 × s, 6 H, C_5*Me*$_4$Ph), 5.17 (d, 1 H, $^3J_{HH}$ = 16.2 Hz, TiCH=C*H*), 5.25 (d, 1 H, $^3J_{HH}$ = 16.2 Hz, Ti*C*H=CH), 6.98−7.17 (m, 10 H, *Ph*). ^{13}C{^{1}H} NMR (C_6D_6): δ 13.3, 14.5 (C_5*Me*$_4$Ph), 28.3 (Me$_3$*C*), 30.3, 31.7 (*Me*$_3$C), 35.6 (Me$_3$*C*), 121.8 (TiC≡*C*), 124.3, 125.1 ($C_5Me_4Ph_5$, *C*Me), 125.7 (C_5Me$_4$-Ph, *C*Ph or Ph, *C*$_{ipso}$), 126.2, 130.4 (C_5Me_4Ph, *C*H of Ph); 136.1 (C_5Me_4Ph, *C*Ph or Ph, *C*$_{ipso}$), 144.2 (TiCH=*C*H), 151.9 (Ti*C*≡C), 193.9 (Ti*C*H=CH). One of the *C*H(Ph) signals is overlapped by the solvent multiplet. UV−near-IR (hexane, nm): 400 (sh) > 470 (sh).

[(η^5-C_5Me_4Bz)$_2$Ti{η^1-(*E*)-CH=CHCMe$_3$}(η^1-C≡CCMe$_3$) (A4). The absorption band of **4** at 920 nm disppeared after 7 h at 60 °C, and the consumption of TBUE ceased at the same time. **A4** formed as a noncrystallizing dark yellow waxy product, yield 0.64 g (ca. 100%). ^{1}H NMR (C_6D_6): δ 1.12, 1.29 (2 × s, 9 H, *Me*$_3$C), 1.78, 1.80, 1.86, 1.90 (4 × s, 6 H, C_5*Me*$_4$-Bz), 3.87 (s, 4 H, PhC*H*$_2$), 4.85 (d, 1 H, $^3J_{HH}$ = 16.5 Hz, TiCH=C*H*), 5.11 (d, 1 H, $^3J_{HH}$ = 16.5 Hz, TiC*H*=CH), 7.03−7.23 (m, 10 H, *Ph*). ^{13}C{^{1}H} NMR (C_6D_6): δ 12.6, 12.6, 13.5, 13.5 (C_5*Me*$_4$-Bz), 28.3 (Me$_3$*C*), 30.4, 31.8 (*Me*$_3$C), 34.6 (Ph*C*H$_2$), 35.5 (Me$_3$*C*), 120.8, 121.2, 121.9, 122.3 (C_5Me_4Bz, *C*Me), 124.6 (TiC≡*C*), 125.3 (Ph, *C*$_{ipso}$), 126.0, 128.5, 128.7 (Ph, *C*H), 142.0 (C_5Me$_4$-Bz, *C*CH$_2$), 143.1 (TiCH=*C*H), 150.1 (TiC≡C), 193.5 (Ti*C*H=CH). UV−near-IR (hexane, nm): 390 (sh) > 480 (sh).

[(η^5-C_5Me_4H)$_2$Ti{η^1-(*E*)-CH=CHSiMe$_3$}(η^1-C≡CSiMe$_3$)] (A5). TMSE (1.1 mL, 8.0 mmol) was added to a solution of **1** (0.46 g, 1.0 mmol) in hexane (20 mL), and the solution was heated to 60 °C. After 4 h the absorption band of **1** at 920 nm disappeared and the absorption band of TMSE at 1540 nm indicated the consumption of ca. 2 mmol of TMSE. **A5** was formed as an orange-yellow waxy solid, yield 0.45 g (93%). ^{1}H NMR (C_6D_6): δ 0.12, 0.19 (2 × s, 9 H, *Me*$_3$Si), 1.56, 1.72, 1.90, 2.20 (4 × s, 6 H, C_5*Me*$_4$H), 4.71 (s, 2 H, C_5Me_4*H*), 5.73 (d, 1 H, $^3J_{HH}$ = 20.5 Hz, TiCH=C*H*), 6.22 (d, 1 H, $^3J_{HH}$ = 20.5 Hz, Ti*C*H=CH). ^{13}C{^{1}H} NMR (C_6D_6): δ −0.4, 0.7 (*Me*$_3$Si), 13.2, 14.1, 14.2, 15.0 (C_5*Me*$_4$H), 109.2 (C_5Me_4H, *C*H), 118.1 (TiC≡*C*), 120.6, 120.7, 126.5, 127.2 (C_5Me_4H, *C*Me), 137.3 (TiCH=*C*H), 181.1 (Ti*C*≡C), 227.6 (Ti*C*H=CH). UV−near-IR (hexane, nm): 405 (sh) > 475(sh).

[(η^5-(C_5Me_4H)$_2$Ti{η^1-(*E*)-CH=CHFc}(η^1-C≡CFc)] (A6). A hexane solution (20 mL) of **1** (0.5 mmol in 3.5 mL) and a toluene solution of FcC≡CH (0.25 g in 6 mL of toluene) were mixed in an ampule equipped with a quartz cell (d = 0.2 cm) and kept in the dark. After 2 days at room temperature, the absorption band at 920 nm of the BTMSE complex disappeared. Addition of 10 mL of hexane resulted in precipitation of a red voluminous precipitate. The yellow mother liquor was separated and the precipitate washed twice with hexane and dried under vacuum. The solid was dissolved in toluene and crystallized by slow evaporation of the solvent to give dark red crystals of **A6** in rich aggregates; yield 0.30 g (83%). The mother liquor contained BTMSE and a trace of HTT dimer (FCE)$_2$. Mp: 85 °C. ^{1}H NMR (C_6D_6): δ 1.61, 1.73, 2.04, 2.31 (4 × s, 6 H, C_5*Me*$_4$H), 3.99, 4.34 (2 × apparent t, 2 H, AA′BB′ of C_5H_4Fe), 4.00, 4.24 (2 × apparent t, 2 H, AA′BB′ of C_5H_4Fe), 4.19, 4.25 (2 × s, 5 H, C_5H_5Fe), 4.81 (s, 2 H, C_5Me_4*H*), 5.72 (d, $^3J_{HH}$ = 17.2 Hz, 1H, TiCH=C*H*), 6.06 (d, $^3J_{HH}$ = 17.2 Hz, 1H, Ti*C*H=CH). ^{13}C{^{1}H} NMR (C_6D_6): δ 13.1, 14.0, 14.1, 14.9 (C_5*Me*$_4$H), 65.7, 67.7 (C_5H_4Fe, *C*H), ca. 67.7 (C_5H_4Fe, *C*$_{ipso}$; overlapped by *C*H of C_5H_4Fe), 68.8 (C_5H_4Fe, *C*H), 69.1, 69.9 (C_5H_5Fe, *C*H), 71.7 (C_5H_4Fe, *C*H), 90.7 (C_5H_4Fe, *C*$_{ipso}$), 109.1 (C_5Me_4H, *C*H), 120.4, 120.4, 127.0, 127.2 (C_5Me_4H, *C*Me), 115.7 (TiC≡*C*), 128.6 (TiCH=*C*H), 160.3 (Ti*C*≡C), 200.8 (Ti*C*H=CH). IR (KBr): 2893 (m), 2053 (m), 1434 (m), 1365 (m), 1221 (m), 1104 (m), 1032 (sh), 1018 (s), 997 (s), 984 (m), 915 (s), 851 (m), 835 (m), 810 (vs), 800 (sh), 652 (m), 631 (m), 580 (m), 531 (m), 483 (vs). UV−near-IR (hexane, nm): 450. Anal. Calcd for $C_{42}H_{46}Fe_2Ti$: C, 71.01; H, 6.53. Found: C, 70.96; H, 6.52.

Photoassisted Synthesis of B Type Complexes. NMR sample tubes (5 mm diameter) containing solutions of compounds **A1**−**A6** in C_6D_6 were exposed to sunlight for various periods (from a few hours to several days), whereupon the yellow color of compounds **A1**−**A5** disappeared and the solutions turned blue or green. The progress in conversion of the **A** type compounds into the titanocene complexes of head-to-head dimers was followed by ^{1}H and ^{13}C NMR spectra, which showed that the conversion proceeds very cleanly, affording quantitatively one product. However, the reaction seems to be autocatalytic, since the reaction times varied widely. This discouraged us from studying the optimum wavelength region and quantum yields of the photolysis. In the absence of light, the samples of **A** type complexes are stable for at least 1 year at room temperature. For preparative purposes compounds **A1**−**A6** were obtained from 1 mmol quantities of **1**−**4** as given above and exposed to sunlight in the form of hexane solutions. The photolysis was continued until the solutions reached the color obtained in NMR tubes. The workup consisted of evaporation of all volatiles and attempted crystallization from concentrated hexane solution. Unfortunately, a crystalline product was obtained for **B1** only; the other complexes formed noncrystallizing oils or waxy solids.

[(η^5-C_5Me_4H)$_2$Ti{η^2-(*E*)-Me$_3$CC≡C(CH=CHCMe$_3$)}] (B1). According to NMR measurements the conversion was practically quantitative; however, the yield of blue crystals of pure **B1** was only 80 mg (18% related to **1**) due to the high solubility of the complex in hexane. Mp: 96 °C. ^{1}H NMR (C_6D_6): δ 0.94, 1.03 (2 × s, 9 H, *Me*$_3$C), 1.36, 1.79, 1.97, 2.08 (4 × s, 6 H, C_5*Me*$_4$H), 4.15 (d, 1 H, $^3J_{HH}$ = 15.4 Hz, CH=C*H*CMe$_3$), 5.85 (s, 2 H, C_5Me_4*H*), 6.17 (d, 1 H, $^3J_{HH}$ = 15.4 Hz, C*H*=CHCMe$_3$). ^{13}C{^{1}H} NMR (C_6D_6): δ 12.8, 13.0, 13.6, 14.3 (C_5*Me*$_4$H), 29.7, 32.6 (*Me*$_3$C), 33.1, 42.1 (Me$_3$*C*), 112.0 (C_5Me_4H, *C*H), 119.8 (C_5-Me$_4$H, *C*Me), 122.5 (CH=*C*HCMe$_3$), 122.6, 123.4, 124.9 (C_5-Me$_4$H, *C*Me), 144.2 (*C*H=CHCMe$_3$), 199.4 (Me$_3$C*C*≡C), 218.0 (Me$_3$CC≡*C*). EI-MS (direct inlet, 70 eV, 90 °C): *m*/*z* (relative abundance) 454 ($M^{\bullet+}$; 5), 292 (10), 291 (27), 290 (100), 289 (22), 288 (16), 167 (9), 166 (7), 164 (12), 57 (6). IR (hexane, cm^{-1}): 1640. UV−near-IR (hexane, nm): 315 > 390 (sh) > 550 ≈ 725. Anal. Calcd for $C_{30}H_{46}Ti$: C, 79.27; H, 10.20. Found: C, 79.31; H, 10.23.

[(η^5-C_5Me_5)$_2$Ti{η^2-(*E*)-Me$_3$CC≡CCH=CHCMe$_3$}] (B2): blue waxy solid, yield 0.41 g (85% related to **2**). ^{1}H NMR (C_6D_6): δ 0.97, 1.12 (2 × s, 9 H, *Me*$_3$C), 1.85 (s, 30 H, C_5Me$_5$), 4.16 (d, 1 H, $^3J_{HH}$ = 15.3 Hz, CH=C*H*CMe$_3$), 6.24 (d, 1 H, $^3J_{HH}$ = 15.4 Hz, C*H*=CHCMe$_3$). ^{13}C{^{1}H} NMR (C_6D_6): δ 12.9 (C_5*Me*$_5$), 29.8 (*Me*$_3$C), 33.1 (Me$_3$*C*), 33.3 (*Me*$_3$C), 42.5 (Me$_3$*C*), 121.7 (C_5*Me*$_5$), 123.1 (CH=*C*HCMe$_3$), 144.0 (*C*H=CHCMe$_3$), 203.9 (Me$_3$C*C*≡C), 218.6 (Me$_3$CC≡*C*). IR (hexane, cm^{-1}): 1627. UV−near-IR (hexane, nm): 540 ≈ 730.

[(η^5-C_5Me_4Ph)$_2$Ti{η^2-(*E*)-Me$_3$CC≡C(CH=CHCMe$_3$)}] (B3): turquoise waxy solid, yield 0.49 g (81% related to **3**). ^{1}H NMR (C_6D_6): δ 0.95, 0.97 (2 × s, 9 H, *Me*$_3$C), 1.90, 1.95, 1.97, 2.19 (4 × s, 6 H, C_5*Me*$_4$Ph), 4.58 (d, 1 H, $^3J_{HH}$ = 15.5 Hz, CH=C*H*CMe$_3$), 6.09 (d, 1 H, $^3J_{HH}$ = 15.5 Hz, C*H*=CHCMe$_3$), 6.57−6.65 (br d, 4 H, Ph), 6.94−7.13 (m, 6 H, Ph). ^{13}C{^{1}H} NMR (C_6D_6): δ 13.0, 13.8, 14.1, 14.9 (C_5*Me*$_4$Ph), 29.8, 32.9 (*Me*$_3$C), 33.2, 43.1 (Me$_3$*C*), 122.7, 123.9 (C_5Me_4Ph, *C*Me), 123.9 (CH=*C*HCMe$_3$), 124.0, 125.0 (C_5Me_4Ph, *C*Me), 125.3 (C_5Me_4Ph, *C*Ph or Ph, *C*$_{ipso}$), 126.0, 129.5 (C_5Me_4Ph, *C*H of Ph), 137.7 (C_5Me$_4$-

Ph, *C*Ph or Ph, C_{ipso}), 142.8 (*C*H=CHCMe$_3$), 205.4 (Me$_3$C*C*≡C), 220.5 (Me$_3$CC≡*C*); one *C*H(Ph) signal is overlapped by the solvent multiplet. IR (hexane, cm^{-1}): 1630. UV−near-IR (hexane, nm): 650.

[{η^5-C$_5$Me$_4$Bz)$_2$Ti{η^2-(*E*)-Me$_3$CC≡CCH=CHCMe$_3$}] (B4): dark green oil, 0.52 g (82% related to **4**). ^{1}H NMR (C$_6$D$_6$): δ 0.97, 1.14 (2 × s, 9 H, *Me*$_3$C), 1.79, 1.82, 1.84, 1.94 (4 × s, 6 H, C$_5$*Me*$_4$Bz), 3.77, 3.85 (2 × d, 2 H, $^2J_{HH}$ = 16.3 Hz, AB of PhC*H*$_2$), 4.26 (d, 1 H, $^3J_{HH}$ = 15.3 Hz, CH=C*H*CMe$_3$), 6.26 (d, 1 H, $^3J_{HH}$ = 15.3 Hz, C*H*=CHCMe$_3$), 6.98−7.32 (m, 10 H, Ph). ^{13}C{^{1}H} NMR (C$_6$D$_6$): δ 12.7, 12.8, 13.1, 13.5 (C$_5$*Me*$_4$Bz), 29.8 (*Me*$_3$C), 33.3 (Me$_3$*C*), 33.5 (*Me*$_3$C), 33.9 (Ph*C*H$_2$), 42.84 (Me$_3$*C*), 121.8, 122.0, 122.6, 123.0 (C$_5$Me$_4$Bz, *C*Me), 123.2 (CH=*C*HCMe$_3$), 125.1 (Ph, C_{ipso}), 126.0, 128.4, 128.7 (Ph, *C*H), 142.30 (C$_5$Me$_4$-Bz, *C*CH$_2$), 144.7 (*C*H=CHCMe$_3$), 204.7 (Me$_3$C*C*≡C), 219.6 (Me$_3$CC≡*C*). IR (hexane, cm^{-1}): 1635. UV−near-IR (hexane, nm): 580 (sh) < 680.

[(η^5-C$_5$Me$_4$H)$_2$Ti{η^2-(*E*)-Me$_3$SiC≡CCH=CHSiMe$_3$} (B5): yellow-green oil, yield 0.39 g (80% related to **1**). ^{1}H NMR (C$_6$D$_6$): δ 0.04, 0.07 (2 × s, 9 H, *Me*$_3$Si), 1.34, 1.40, 2.12, 2.16 (4 × s, 6 H, C$_5$*Me*$_4$H), 4.59 (d, 1 H, $^3J_{HH}$ = 18.3 Hz, CH=C*H*SiMe$_3$), 4.89 (s, 2 H, C$_5$Me$_4$*H*), 6.53 (d, 1 H, $^3J_{HH}$ = 18.3 Hz, C*H*=CHSiMe$_3$). ^{13}C{^{1}H} NMR (C$_6$D$_6$): δ −1.1, 3.1 (2 × s, 9 H, *Me*$_3$Si), 13.4, 13.5, 13.6, 13.7 (C$_5$*Me*$_4$H), 112.4 (C$_5$Me$_4$H, *C*H), 120.0, 120.4, 125.1, 126.5 (C$_5$Me$_4$H, *C*Me), 132.1 (CH=*C*HSiMe$_3$), 142.5 (*C*H=CHSiMe$_3$), 222.5 (Me$_3$Si*C*≡C), 231.5 (Me$_3$SiC≡*C*). IR (hexane, cm^{-1}): 1645. UV−near-IR (hexane, nm): 540 (sh) > 700 (b).

[(η^5-C$_5$Me$_4$H)$_2$Ti(η^2-(*E*)-FcC≡CCH=CHFc)] (B6): red oil adhering on glass walls, yield ca. 0.4 g (56%). ^{1}H NMR (C$_6$D$_6$): δ 1.42, 1.51, 2.12, 2.23 (4 × s, 6 H, C$_5$Me$_4$H), 3.71, 3.99 (2 × apparent t, 2 H, AA′BB′ of C$_5$*H*$_4$Fe), 4.09, 4.37 (2 × apparent t, 2 H, AA′BB′ of C$_5$*H*$_4$Fe), 4.14, 4.24 (2 × s, 5 H, C$_5$*H*$_5$Fe), 5.04 (s, 2 H, C$_5$Me$_4$*H*), 5.39 (d, $^3J_{HH}$ = 15.4 Hz, 1 H, CH=C*H*Fc), 7.13 (d, $^3J_{HH}$ = 15.4 Hz, 1 H, C*H*=CHFc). ^{13}C{^{1}H} NMR (C$_6$D$_6$): δ 13.4, 13.5, 13.6, 13.7 (C$_5$*Me*$_4$H), 66.7, 67.2, 68.5, 69.0 (C$_5$H$_4$Fe, *C*H), 69.3, 69.4 (C$_5$*H*$_5$Fe), 85.9, 89.2 (C$_5$H$_4$Fe, C_{ipso}), 112.3 (C$_5$Me$_4$H, *C*H), 120.1, 120.3, 126.3, 126.7 (C$_5$Me$_4$H, *C*Me), 126.4 (CH=*C*HFc), 129.4 (*C*H=CHFc), 204.4 (Fc*C*≡C), 209.97 (FcC≡*C*). IR (hexane, cm^{-1}): 1620, 1640. UV−near-IR (hexane, nm): 440 ≫ 650 (b).

Synthesis of Titanocene Complexes with η^2-Coordinated HTT Dimers. Titanocene dichlorides [(η^5-C$_5$Me$_4$R)$_2$-TiCl$_2$] (R = H, Me, Ph; 1.0 mmol) were reduced by a 10−50-fold molar excess of magnesium metal in THF (20 mL) in the presence of Me$_3$SiC≡CC(SiMe$_3$)=CH$_2$ (0.7 mL, 5.0 mmol) at 60 °C. With commercial magnesium turnings (Aldrich for Grignard reagents), induction periods did not exceed 2 h, but with magnesium recovered from previous reductions under vacuum conditions, the reduction began immediately and was completed within 30 min. The resulting solution was separated from excess magnesium and evaporated under vacuum overnight. The residue was extracted by hexane to give brown-yellow solutions from which the **D** type complexes were crystallized.

[(η^5-C$_5$Me$_4$H)$_2$Ti{3,4-η-Me$_3$SiC≡CC(SiMe$_3$)=CH$_2$}] (D1): yellow-brown crystalline material, yield 0.32 g (66%). ^{1}H NMR (C$_6$D$_6$): δ −0.10, 0.15 (2 × s, 9 H, *Me*$_3$Si), 1.03, 1.88, 1.90, 1.93 (4 × s, 6 H, C$_5$*Me*$_4$H), 3.13, 5.04 (2 × d, 1 H, $^2J_{HH}$ = 4.5 Hz, AB of =C*H*$_2$), 5.83 (s, 2 H, C$_5$Me$_4$*H*). ^{13}C{^{1}H} NMR (C$_6$D$_6$): δ −0.4, 3.8 (2 × *Me*$_3$Si), 12.4, 12.7, 14.4, 14.5 (C$_5$*Me*$_4$H), 112.7 (C$_5$Me$_4$H, *C*H), 121.0, 123.8, 124.5, 125.4 (C$_5$Me$_4$H, *C*Me), 130.7 (=*C*H$_2$), 150.3 (=C(SiMe$_3$)-), 208.7 (Me$_3$Si*C*≡C), 216.1 (Me$_3$SiC≡*C*). ^{29}Si DEPT (C$_6$D$_6$): −21.2 (s, C≡C*Si*Me$_3$), −4.3 (s, C=C*Si*Me$_3$). MS (direct inlet, 70 eV, 130−140 °C): *m*/*z*(relative abundance) 486 (M$^{\bullet+}$; 0.1), 327 (5), 325 (13), 309 (6), 292 (5), 291 (13), 290 ([M − (TMSA)$_2$]$^+$; 46), 289 (25), 288 (15), 287 (11), 286 (6), 285 (7), 204 (6), 203 (5), 197 (7), 196 ([(TMSA)$_2$]$^+$; 31)), 183 (7), 182 (15), 181 (72), 168 (6), 167 (9), 166 (8), 165 (6), 164 (8), 163 (6), 157 (7), 156 (15), 155 (82), 108 (26), 105 (8), 97 (9), 83 (9), 74 (8), 73 (100), 70 (10), 45 (17), 43 (11). IR (hexane, cm^{-1}): 1670 (s), 1646 (m), 1245 (vs), 1180 (m), 1020 (m), 947 (s), 915 (m), 840 (vs,b), 746 (s). UV−near-IR (hexane, nm): 500 (sh) ≈ 910.

[(η^5-C$_5$Me$_5$)$_2$Ti{3,4-η-Me$_3$SiC≡CC(SiMe$_3$)=CH$_2$}] (D2): yellow-brown crystals, yield 0.68 g (76%). ^{1}H NMR (C$_6$D$_6$): δ 0.02, 0.18 (2 × s, 9 H, *Me*$_3$Si), 1.76 (s, 30 H, C$_5$*Me*$_5$), 2.88, 5.12 (2 × d, 1 H, $^2J_{HH}$ = 4.6 Hz, AB of =C*H*$_2$). ^{13}C{^{1}H} NMR (C$_6$D$_6$): δ 0.2, 5.5 (2 × *Me*$_3$Si), 12.9 (C$_5$*Me*$_5$), 122.2 (*C*$_5$Me$_5$), 133.3 (=*C*H$_2$), 149.3 (=C(SiMe$_3$)−), 205.9 (Me$_3$Si*C*≡C), 219.4 (Me$_3$SiC≡*C*). ^{29}Si DEPT (C$_6$D$_6$): −20.5 (s, C≡C*Si*Me$_3$), −4.1 (s, C=C*Si*Me$_3$). MS (direct inlet, 70 eV, 140−150 °C): *m*/*z* (relative abundance) M$^{\bullet+}$ not observed; 337 (7), 320 (9), 319 (26), 318 ([*M* − (TMSA)$_2$]$^+$; 89), 317 (33), 316 (23), 315 (9), 314 (7), 313 (7), 301 (6), 299 (6), 197 (8), 196 (33), 183 (8), 182 (19), 181 (88), 180 (6), 179 (6), 178 (10), 177 (7), 176 (5), 157 (9), 156 (19), 155 (91), 119 (9), 108 (27), 97 (10), 83 (9), 74 (8), 73 (100), 70 (11), 45 (17). IR (KBr, cm^{-1}): 2950 (s,b), 2887 (s,b), 2848 (m), 1658 (s), 1630 (m), 1430 (s,b), 1374 (s), 1240 (vs), 1019 (m), 935 (s), 920 (m), 833 (vs,b), 747 (s), 700 m), 671 (m), 643 (m), 440 (m). UV−near-IR (hexane, nm): 400(sh) ≫ 510 (sh) ≈ 925. Anal. Calcd for C$_{30}$H$_{50}$Si$_2$Ti: C, 70.00; H, 9.79. Found: C, 70.03; H, 9.80.

[(η^5-C$_5$Me$_4$Ph)$_2$Ti{3,4-η-Me$_3$SiC≡CC(SiMe$_3$)=CH$_2$}] (D3): dark yellow crystalline material, yield 0.47 g (74%). ^{1}H NMR (C$_6$D$_6$): δ 0.04, 0.18 (2 × s, 9 H, *Me*$_3$Si), 1.79, 1.88, 2.11, 2.17 (4 × s, 6 H, C$_5$*Me*$_4$Ph), 3.62, 5.22 (2 × d, 1 H, $^2J_{HH}$ = 4.4 Hz, =C*H*$_2$), 6.27 (br d, 4 H, *J* = 7.1 Hz, *Ph*), 6.89−7.02 (m, 6 H, *Ph*). ^{13}C NMR (C$_6$D$_6$): δ 0.42, 5.13 (*Me*$_3$Si), 13.9, 14.3, 14.3, 14.6 (C$_5$*Me*$_4$Ph), 122.1, 123.2 (C$_5$Me$_4$Ph, *C*Me), 125.9 (Ph, *C*H), 126.6, 127.2 (C$_5$Me$_4$Ph, *C*Me), 127.7, 128.9 (Ph, *C*H), 132.7 (=*C*H$_2$), 137.3 (C$_5$Me$_4$Ph, *C*Ph or Ph, C_{ipso}), 150.0 (*C*=CH$_2$), 209.1 (η^2-Me$_3$Si*C*≡C), 221.2 (η^2-Me$_3$SiC≡*C*). One of the Ph, C_{ipso} and C$_5$Me$_4$Ph, *C*Ph signals was not found due to its overlap with the solvent resonance. MS (direct inlet, 70 eV, 145−155 °C): *m*/*z* (relative abundance) M$^{\bullet+}$ not observed; 444 (14), 443 (40), 442 ([(C$_5$Me$_4$Ph)$_2$Ti]$^+$; 100), 441 (34), 440 (19), 439 (6), 242 (5), 241 (5), 240 (5), 221 (5), 196 (10), 181 (16), 165 (5), 155 (14), 73 (27). IR (KBr): 1635−1655 cm^{-1}. UV−near-IR (hexane, nm): 910.

Analogous reduction of [(η^5-C$_5$Me$_5$)$_2$TiCl$_2$] in the presence of Me$_3$CC≡CC(CMe$_3$)=CH$_2$ gave after the usual workup a purple paramagnetic solution which contained the "tucked in" compound [(η^1:η^5-C$_5$Me$_4$CH$_2$)(η^5-C$_5$Me$_5$)Ti] according to MS and EPR spectra.[19] Under the same conditions, [(η^5-C$_5$Me$_4$H)$_2$TiCl$_2$] afforded a complicated mixture in which the [(η^5-C$_5$Me$_4$H)$_2$Ti-{η^2-Me$_3$CC≡CC(CMe$_3$)=CH$_2$}] complex was detected by NMR spectroscopy.

Reactivity Experiments. Reaction between 1 and TBUE Assisted by Sunlight. A hexane solution of **1** (90 mg, 0.2 mmol in 4.9 mL) and TBUE (2.6 mL, 21.2 mmol) were mixed in an ampule equipped with a pair of 1.0 and 0.1 cm quartz cells. After 4.5 h in the dark, the concentration of the BTMSE complex decreased to 90% of the initial value while the concetration of TBUE remained virtually unchanged within the precision of the measurement. However, after 2 h in sunlight the concentration of the BTMSE complex decreased to 62% of its initial value and TBUE was consumed completely. When more TBUE (1.5 mL, 12 mmol) was added, this was consumed after another 2 h of exposure to sunlight and the amount of the BTMSE complex decreased to ca. 20% of the original amount. This corresponds to a turnover number (TN) of 210 molecules of TBUE per molecule of **1**.

Reaction between 2 and TMSE Assisted by Sunlight. A hexane solution of **2** (98 mg, 2 mmol in 2.0 mL) and TMSE (3.0 mL, 21.2 mmol) were mixed in an ampule equipped with a pair of 1.0 and 0.1 cm quartz cells. After 2 h in the dark the concentration of **2** decreased to 91% and a corresponding decrease of the TMSE concentration ranged the precision of the measurement. Upon exposure to direct sunlight for 2 h, however, the concentration of **2** and TMSE decreased to 50% and to about 2% of their initial values, respectively. This

Table 6. Crystallographic Data, Data Collection and Structure Refinement for A1, A6, B1, and D2

	A1	A6	B1	D2[a]
formula	$C_{30}H_{46}Ti$	$C_{42}H_{46}Fe_2Ti$	$C_{30}H_{46}Ti$	$C_{30}H_{50}Si_2Ti$
M_r	454.57	710.39	454.57	514.78
cryst syst	monoclinic	monoclinic	monoclinic	orthorhombic
space group	*C*2/*c*	$P2_1/n$	$P2_1/n$	$P2_12_12_1$
T (K)	100(1)	294(1)	294(1)	294(1)
a (Å); α (deg)	14.383(3); 90	15.868(3); 90	17.533(2); 90	10.036(2); 90
b (Å); *β* (deg)	11.172(2); 113.46(1)	10.553(2); 102.03(1)	9.5876(9); 115.747(8)	16.101(3); 90
c (Å); *γ* (deg)	18.575(3); 90	20.881(3); 90	18.183(1); 90	19.030(3); 90
V (Å^3); *Z*	2738.0(9); 4	3419.9(9); 4	2753.0(3); 4	3075(1); 4
2*θ* range for cell param determn (deg)	30−32	26−28	26−28	26−28
D_c (g mL^{-1})	1.10	1.38	1.10	1.11
cryst size (mm^3)	0.30 × 0.30 × 0.40	0.25 × 0.32 × 0.39	0.20 × 0.35 × 0.35	0.46 × 0.68 × 0.79
cryst descripn	yellow bar	orange-red fragment	blue bar	red-brown prism
μ(Mo Kα) (mm^{-1})	0.326	1.09	0.325	0.372
F(000)	992	1488	992	1120
2*θ* range (deg); *hkl*	4.8−51.9; +*h*,+*k*,±*l*	2.9−49.9; ±*h*,+*k*,+*l*	2.7−44.0; +*h*,+*k*,±*l*	3.3−49.9; ±*h*,±*k*,±*l*
vari in stds[b]	9.8	5.8	2.1	2.4
no. of diffractions collected; *R*(*σ*)[c]	2795; 1.91	6190; 11.0	3491; 13.2	4732; 2.23
no. of unique diffractions	2693	6009	3369	4391
no. of diffractions obsd; $F_o \geq 4\sigma(F_o)$	2341	3360	1819	3973
weighting scheme: w_1; w_2[d]	0.0948; 3.6836	0.0682; 4.7108	0.0517; 0.0423	0.0567; 0.2158
no. of params	254	466	311	304
$R_{all}(F)$; $R_{obsd}(F)$ (%)[c]	5.25; 4.22	15.1; 5.73	15.8; 4.94	3.98; 3.05
$R_{w,all}(F^2)$; $R_{w,obsd}(F^2)$ (%)[c]	12.8; 12.0	16.4; 13.8	12.1; 9.80	8.42; 8.04
GOF_{all}[c]	0.899	1.04	1.00	1.08
Δ*ρ* (e Å^{-3})	0.80; −0.31	0.49, −0.33	0.21; −0.24	0.18; −0.41

[a] Flack's absolute structure parameter $x = 0.00(2)$. [b] Three standard diffractions were monitored every 1 h in all cases. [c] $R(\sigma) = \sum\sigma(F_o^2)/\sum F_o^2$, $R(F) = \sum||F_o| - |F_c||/\sum|F_o|$, $R_w(F^2) = [\sum(w(F_o^2-F_c^2)^2)/(\sum w(F_o^2)^2)]^{1/2}$, GOF $= [\sum(w(F_o^2-F_c^2)^2)/(N_{diffrs}-N_{params})]^{1/2}$. [d] Weighting scheme: $w = [\sigma^2(F_o^2) + (w_1P)^2 + w_2P]^{-1}$, where $P = {}^1/_3[\max(F_o^2) + 2F_c^2]$.

corresponds to the conversion of 210 molecules of TMSE per molecule of the converted BTMSE complex. Another 3.0 mL of TMSE was added, and the mixture was exposed to full sunlight for another 1 h. As a result, the amount of **2** decreased to 25% of the original value and all TMSE dimerized. In all, 0.15 mmol of **2** converted a total of 42.4 mmol of TMSE, which gives a TN value of 283.

Conversion of D2 into A2 and B2. Complex **D2** obtained as described above (ca. 1.0 mmol) in hexane (10 mL) was mixed with TBUE (1.0 mL, 8.1 mmol) in the dark at room temperature. The absorption band of **D2** at 925 nm decayed within 30 min, while the yellow color of the solution did not change. The usual workup gave a yellow crystalline solid whose NMR spectra were identical with those of **A2**. The volatiles evaporated under vacuum showed the ratio of HTT dimers $(TBU)_2$/$(TMSE)_2$ ca. 2:1. After exposure of **A2** in C_6D_6 to sunlight it rapidly turned into **B2**, as shown by NMR and UV−near-IR spectra.

Reaction of D2 with TMSE. A solution of **D2** in hexane (0.1 mmol in 2 mL) in an ampule equipped with a quartz cell (0.1 cm) was mixed with 2.5 mL of TMSE (17.7 mmol) in diffuse daylight. Within 10 min after mixing, the absorption bands of **D2** (925 nm) and of TMSE (1640 nm) were not observable. Then another portion of TMSE (2.0 mL, 14.2 mmol) was added; this was consumed within 10 min. The volatiles were removed, and GC-MS analysis revealed in addition to hexane only the HTT dimer $(TMSE)_2$ (TN = 319).

Reaction of B1 with TBUE. A solution of **B1** from an NMR tube (ca. 0.2 mmol of **B1**) was evaporated, the residue was redissolved in hexane (4.0 mL), and the hexane solution was mixed with TBUE (2.0 mL, 16.2 mmol) in the dark at room temperature. Immediately after addition the blue solution turned brown-yellow and the UV−near-IR spectrum did not show absorption bands at wavelengths longer than 550 nm. All TBUE was consumed within 3 h in the dark (TN = 81).

Reaction of B2 with TMSE. A solution of **B2** from an NMR tube (ca. 0.4 mmol of **B2**) was evaporated, the residue was dissolved in hexane (6.0 mL), and the solution was treated with TMSE (3 mL, 24.0 mmol) in the dark. Immediately after addition, the green solution of **B4** turned orange and TMSE was slowly consumed (to 87% of its initial content during 3.5 h in the dark). After exposure to sunlight for 20 min, all the remaining TMSE was converted to its HTT dimer (TN = 60) and the color of the reaction mixture changed from orange to yellow.

Reaction of B1 with BTMSE. Crystalline **B1** (0.050 g, 0.11 mmol) was dissolved in hexane (4.0 mL), and BTMSE (0.1 mL, 0.45 mmol) was added. The electronic absorption spectrum of **B1** was replaced by the spectrum of **1**, dominated by the absorption band at 920 nm after standing overnight.

Reaction of D2 with BTMSE. Crystalline **D2** (0.20 g, 0.39 mmol) was dissolved in hexane (5.0 mL), and BTMSE (0.1 mL, 0.45 mmol) was added. After 1 h at room temperature the concentration of **D2** decreased by less than 10%, as indicated by a decrease in intensity of the shoulder at 500 nm. After the temperature was raised to 60 °C for 1 h, the above-mentioned shoulder disappeared completely and the solution turned yellow. The GC-MS analysis of volatiles revealed a molar ratio of the HTT dimer $(TMSE)_2$ and BTMSE of 6.5/1. A yellow crystalline residue was identified by an IR spectrum in KBr pellet to be pure complex **2**.

Structure Determination. General Comments. Crystals suitable for X-ray analyses were grown by slow cooling or slow evaporation from hexane (**A1**, **B1**, **D2**) or toluene (**A6**) solutions in evacuated ampules. The selected crystals were inserted into Lindemann glass capillaries and sealed by wax under nitrogen in a glovebox. Diffraction intensities were measured on a CAD4-MACHIII four-circle diffractometer with Mo Kα radiation (λ = 0.710 69 Å) and $\theta-2\theta$ scan mode. An Oxford Cryostream low-temperature device was used for the case of complex **D2**. The cell parameters were determined by least squares from 25 automatically centered diffractions selected within 2*θ* ranges given in Table 6. No absorption correction was applied. The structures have been solved by direct methods (SIR92[35]) and refined by full-matrix least squares on weighted F^2 (SHELXL97[36]). Some relevant crystallographic

(35) Altomare, A.; Burla, M. C.; Camalli, M.; Cascarano, G.; Giacovazzo, C.; Guagliardi, A.; Polidori, G. *J. Appl. Crystallogr.* **1994**, *27*, 435.

(36) Sheldrick, G. M. SHELXL97: Program for Crystal Structure Refinement from Diffraction Data; University of Göttingen: Göttingen, Germany, 1997.

data are given in Table 6. Structural data for all compounds were deposited at the Cambridge Crystallographic Data Centre and are also available as Supporting Information. Thermal ellipsoid plots were drawn by the PLATON92[37] program.

Crystal Structure of A1. The refinement in the noncentrosymmetric space group *Cc* proved unstable due to high correlations of the parameters since the Ti−*C*≡*C* and Ti−*CH*═*CH* moieties that only violate the virtual 2-fold symmetry of the molecule are randomly distributed throughout the lattice. Hence, the calculation was carried out in the related centrosymmetric space group *C*2/*c*, where the alkynyl and alkenyl moieties were refined each with equal probability over the two positions related by the crystallographic 2-fold symmetry axis (-*x*, *y*, $^1/_2 - z$) (Ti is located in a special position (0, *y*, $^1/_4$) with $y = 0.21905(4)$). Furthermore, the methyls of both *tert*-butyl groups exhibit an extensive rotational disorder along the pivotal *C*−*C*(*t*-Bu) bonds, resulting in an almost toroidal electron density distribution. Two sets of methyl groups were refined for both *tert*-butyl substituents as ideal tetrahedra (*CCH*$_3$) with C−C−H angles of 109.5°, C−H bond lengths of 0.96 Å and $U_{iso}(H) = 1.2[U_{eq}(C)]$. All other hydrogen atoms were identified from difference electron density maps and freely isotropically refined. It is worth noting that a similar statistical disorder of hydrocarbyl ligands has been reported for [(η^5-C_5Me_5)$_2$Ti(η^1-C≡CPh)(η^1-CH═CHPh)].[9]

Crystal Structure of A6. The two double-bond hydrogen atoms were found on the difference electron density map and isotropically refined. Other hydrogen atoms were handled as follows: ferrocene hydrogens were fixed so that the C−H bond of 0.93 Å bisects the outer C−C−C angle of the aromatic ring and their U_{iso} values were freely refined. All methyl hydrogens were attributed ideal tetrahedral geometry (C−C−H angles of 109.5° and C−H bond lengths of 0.96 Å) and in this arrangement isotropically refined by being allowed to rotate freely around the pivotal C−C bond to fit the electron density maxima.

Crystal Structure of B1. For compoud **B1**, an empirical correction for exctinction was applied during the structure refinement as implemented in SHELX97; i.e., the calculated structure factors F_c were multiplied by $k[1 + 0.001xF_c^2\lambda^3(\sin 2\theta)^{-1}]^{-1/4}$, where k is the overall scaling factor, λ the wavelength, and θ the diffraction angle. The refined x value was 0.0015(4). Hydrogen atoms of the double bond and those of cyclopentadienyl CH groups were identified on the difference electron density maps and isotropically refined. Methyl groups on the titanocene cyclopentadienyls as well as those of *tert*-butyl groups were treated in the same manner as for **A6**.

Crystal Structure of D2. The methyl hydrogens in $SiMe_3$ groups and on cyclopentadienyl ligands were treated like those in **A6** but with $U_{iso}(H) = 1.2[U_{eq}(C)]$; the ═C*H*$_2$ hydrogens were identified on an electron density map and isotropically refined.

Acknowledgment. This research was supported by the Grant Agency of the Czech Republic (Grant No. 203/99/0846) and by the Volkswagen Stiftung. The Grant Agency of the Czech Republic sponsored access to the Cambridge Structure Database (Grant No. 203/99/0067).

Supporting Information Available: Tables of crystallographic data, atomic coordinates, thermal parameters, and interatomic and interplanar distances and angles and packing diagrams for **A1**, **A6**, **B1**, and **D2**. This material is available free of charge via the Internet at http://pubs.acs.org.

OM9905714

(37) Spek, A. L. *Acta Crystallogr.* **1990**, *A46*, C34.